NRL Report 8492

Coupled Amplifier Module Feed Networks for Phased Array Antennas

RICHARD A. STEINBERG

Electromagnetics Branch
Radar Division

May 25, 1983

NAVAL RESEARCH LABORATORY
Washington, D.C.

SECURITY CLASSIFICATION OF THIS PAGE *(When Data Entered)*

REPORT DOCUMENTATION PAGE		READ INSTRUCTIONS BEFORE COMPLETING FORM
1. REPORT NUMBER NRL Report 8492	2. GOVT ACCESSION NO.	3. RECIPIENT'S CATALOG NUMBER
4. TITLE *(and Subtitle)* COUPLED AMPLIFIER MODULE FEED NETWORKS FOR PHASED ARRAY ANTENNAS		5. TYPE OF REPORT & PERIOD COVERED Interim report on a continuing NRL problem. 6. PERFORMING ORG. REPORT NUMBER
7. AUTHOR(s) Richard A. Steinberg		8. CONTRACT OR GRANT NUMBER(s)
9. PERFORMING ORGANIZATION NAME AND ADDRESS Naval Research Laboratory Washington, DC 20375		10. PROGRAM ELEMENT, PROJECT, TASK AREA & WORK UNIT NUMBERS 61153N; RR0210543 53-1783-0-3
11. CONTROLLING OFFICE NAME AND ADDRESS Office of Naval Research Washington, DC 22217		12. REPORT DATE May 25, 1983 13. NUMBER OF PAGES 45
14. MONITORING AGENCY NAME & ADDRESS*(if different from Controlling Office)*		15. SECURITY CLASS. *(of this report)* UNCLASSIFIED 15a. DECLASSIFICATION/DOWNGRADING SCHEDULE

16. DISTRIBUTION STATEMENT *(of this Report)*

Approved for public release; distribution unlimited.

17. DISTRIBUTION STATEMENT *(of the abstract entered in Block 20, if different from Report)*

18. SUPPLEMENTARY NOTES

19. KEY WORDS *(Continue on reverse side if necessary and identify by block number)*

Antennas
Arrays
Electronic scan

20. ABSTRACT *(Continue on reverse side if necessary and identify by block number)*

The coupled amplifier module (CAM) lattice is a new type of feed for phased-array antennas that uses far fewer phase shifters than conventional feeds. For example, the CAM feed network for a linear array employs just one phase-shifter; a 2-D rectangular array requires just three phase-shifters.

The CAM feed is realized as a periodic lattice of hard-limited amplifiers. Analysis and computer simulation show that the network establishes a linear phase progression. The CAM network's transient response and sensitivity to fabricational imperfections are also analyzed.

DD FORM 1 JAN 73 1473 EDITION OF 1 NOV 65 IS OBSOLETE
S/N 0102-014-6601

SECURITY CLASSIFICATION OF THIS PAGE *(When Data Entered)*

CONTENTS

COUPLED AMPLIFIER MODULE FEED NETWORKS FOR PHASED ARRAY ANTENNAS

INTRODUCTION AND SUMMARY OF RESULTS

The high cost of phased-array antennas prevents their use in many applications where electronic scanning could provide large performance improvements relative to mechanically scanned antennas. One reason for the high cost of conventional phased-arrays is their parallel construction: each radiating element has its own phase control. Previous approaches to reducing system cost by even modest reductions in the number of phase-shifters result in objectionable increases in sidelobe levels [1]. Although the feed networks discussed in this report allow for greatly reduced numbers of phase-shifters, there are other components that must be added. Thus the cost-effectiveness of the new approach is an issue for further study.

Figure 1 depicts a linear array corporate feed, illustrating the one phase-shifter/element requirement that characterizes conventional design [2]. Figure 2 shows the functionally equivalent coupled amplifier module (CAM) feed. Phase control is provided only at the edges of the CAM feed, and requires just one phase shifter. As shown in Fig. 3, each module in the CAM feed consists of a hard-limited amplifier whose input is the sum of sampled outputs from the two adjacent modules.

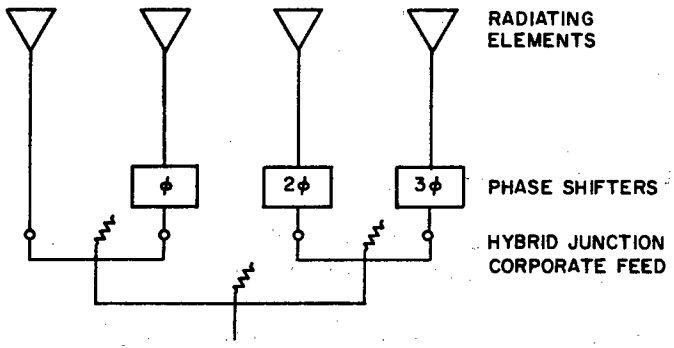

Fig. 1 — Four-element linear array employing conventional hybrid junction corporate feed (3 phase-shifters)

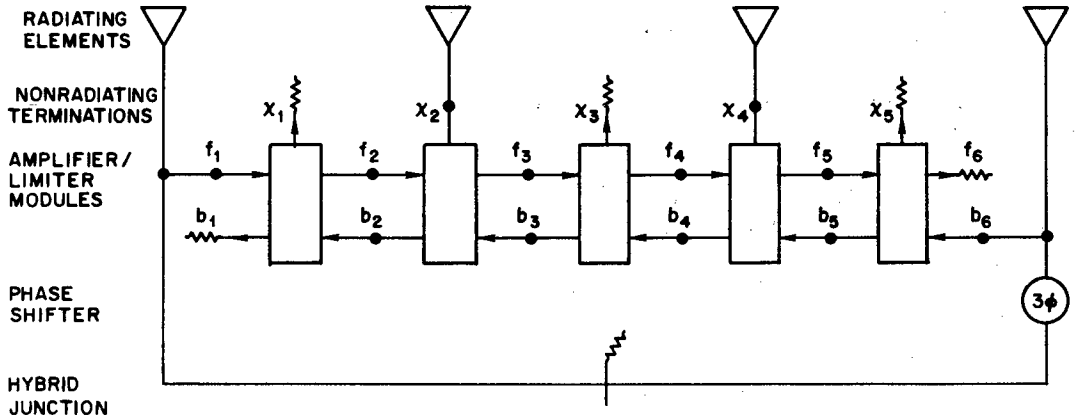

Fig. 2 — Four-element linear array employing coupled amplifier module feed

Manuscript approved November 8, 1982.

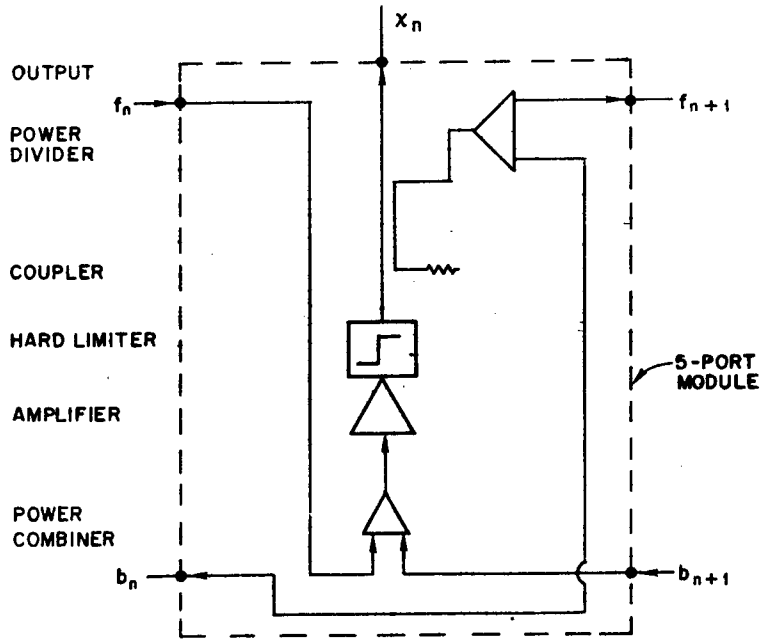

Fig. 3 — Amplifier/limiter module for coupled amplifier module feed

Since the outputs of the amplifier/limiter modules are all of unit amplitude, all information is contained in their phases, $\theta_n(\tau)$, where n is the module index and τ is the time. It is shown that the dynamics of the CAM network are governed by a simple diffusion equation on the phases $\theta_n(\tau)$.

The main body of this report is devoted to developing solutions to the phase diffusion equation. Consideration is given to:

- steady-state phase distributions for fabricationally perfect modules, i.e., modules for which the power dividers effect exactly equal two-way power division;
- the complete transient phase distribution for perfect modules; and
- steady-state phase distributions for fabricationally imperfect modules, including those for which the imperfection can only be characterized statistically.

The phase diffusion equation can be solved exactly when the modules are fabricationally perfect, with the following results.

- While the CAM network establishes a linear phase progression in the steady state, the phase difference between the outputs of adjacent modules is limited to the interval [0°, 90°). If the phase gradient were ever to reach 90° per module, the signals summed at the input to the hard-limited amplifier would be 180° out of phase and therefore would add to zero. Since it is thus impossible to develop phase gradients greater than ±90° per module, two modules/element are required to achieve full hemispheric scanning capability (cf. Fig. 2). (Only one module per element may be required for limited scan applications, however.)
- The exact transient response takes the form of a modal expansion in which each of the spatial modes has a characteristic decay time. Since the transient response is dominated by the spatial

mode having the slowest decay time, a simple and highly accurate one-mode-approximation results.

- The settling time of the CAM network increases as the square of the number of modules. Thus, satisfaction of bandwidth requirements may necessitate introducing additional "speed-up" phase shifters spaced at regular intervals along the feed network.

The analysis for fabricationally imperfect modules permits only approximate solutions for the steady-state phase distributions. Defining the phase gradient error as the difference between the actual phase gradient and the ideal constant gradient, an expression is developed for the phase gradient error for arbitrarily nonuniform CAM structures. Assuming that the nonuniformities from one module to the next are independent, equal-variance random variables, an expression for the root-mean-square (RMS) phase gradient error is then derived. It follows from this analysis that the RMS phase gradient error increases as the square root of the number of modules in the CAM network; also, the error is proportional to tan $\Delta\phi$, where $\Delta\phi$ is the nominal phase increment per module. An example is given for a 9-module feed for which a 1% RMS error in the power splits gives rise to about a 1° RMS phase gradient error, for an assumed nominal phase gradient of 45° per module.

Finally, it is shown that the CAM technique can be applied to 2-D antenna arrays. The CAM feed network for a 2-D rectangular array of arbitrary size requires just three phase-shifters.

In most practical antennas the amplifier/limiter modules feeding the radiating elements would be followed by power RF amplifiers. In receive mode, the coupled module structure would be used as a local oscillator chain to convert the antenna outputs to intermediate frequency (IF).

MODEL FORMULATION

Figure 4 shows an idealized model for the individual amplifier/limiter modules. The principal idealization is in representing the hard limiter as a time-variable amplifier whose gain $N_n(\tau)$ automatically adjusts itself to provide a unit amplitude output, i.e.,

$$x_n(\tau) = \exp j\theta_n(\tau), \tag{1}$$

where n is the module index, and the normalized time τ is defined as

$$\tau = (t/T),$$

where T is the delay time per module (cf. Fig. 4). The gain $N_n(\tau)$ is a function of time and is generally different from one module to the next,

$$N_n(\tau) \neq N_m(\tau), \quad n \neq m. \tag{2}$$

We preserve sinusoidal waveforms by implicitly assuming that the hard limiter in Fig. 3 is followed by a high-Q tuned circuit.

The gains B_{n-1} and F_{n+1} in Fig. 4 are determined from the power splits effected by the two power dividers in Fig. 3 and are respectively referred to as the backward- and forward-coupling coefficients. We generally design the power splitters to achieve the ideal,

$$B_n = F_n. \tag{3}$$

Departures from the ideal are unfortunately inevitable due to fabricational imperfections in the power splitters.

From Figs. 2 and 4,

$$x_n(\tau + 1) = N_n(\tau)[B_n x_{n+1}(\tau) + F_n x_{n-1}(\tau)].$$

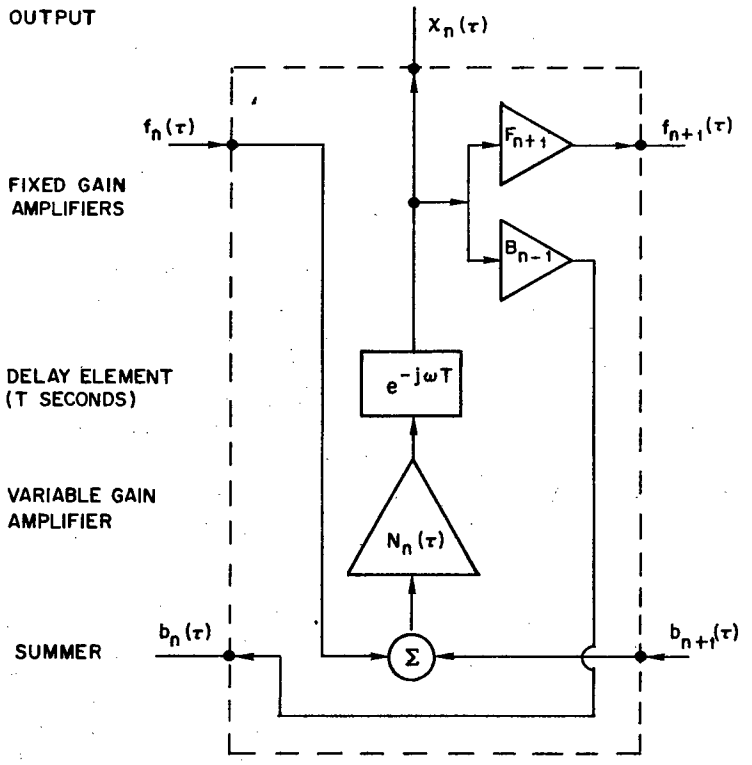

Fig. 4 — Idealized model of amplifier/limiter module depicted in Fig. 3

Thus, from Eq. (1),

$$e^{j\theta_n(\tau+1)} = N_n(\tau)[B_n e^{j\theta_{n+1}(\tau)} + F_n e^{j\theta_{n-1}(\tau)}] \tag{4}$$

where $n = 1, 2, \ldots (M-1)$. Solution of Eq. (4) generally requires the specification of boundary phases at $n = 0$ and $n = M$,

$$\theta_0(\tau) = 0 \tag{5a}$$

$$\theta_M(\tau) = \begin{cases} \theta_M^i = M\Delta\phi_0 - r \cdot 2\pi, & \tau < 0 \\ \theta_M^f = M\Delta\phi - s \cdot 2\pi, & \tau \geqslant 0, \end{cases} \tag{5b}$$

and the initial phases

$$\theta_n(\tau) = \theta_n^i \ , \quad n = 1, 2, \ldots M, \quad \tau < 0. \tag{6}$$

The terms $r \cdot 2\pi$ and $s \cdot 2\pi$ appearing in Eq. (5b), where r and s are integers, reflect the fact that the phase difference $(\theta_M - \theta_0)$ established by the phase-shifter (cf. Fig. 2) is physically determinate only to within an integral multiple of 2π. Also, we note that the number of modules in the feed network is equal to $(M-1)$. (For example, $M = 6$ for the network depicted in Fig. 2.)

For future use we define the quantity $\alpha_M(0)$ as the step change in boundary phasing imposed by the phase-shifter at $\tau = 0$,

$$\alpha_M(0) = \mathrm{mod}_{2\pi}(\theta_M^f - \theta_M^i) = M(\Delta\phi - \Delta\phi_0). \tag{7}$$

The function $mod_{2\pi}(\cdot)$ appearing in Eq. (7) expresses its argument in modulo -2π, i.e., as a number between 0 and 2π.

THE PHASE DIFFUSION EQUATION

It is shown in Appendix A that Eq. (4) can be recast as

$$\theta_n(\tau + 1) = \frac{1}{2}\left\{\theta_{n+1}(\tau) + \theta_{n-1}(\tau) - \epsilon_n \tan \frac{1}{2}[\theta_{n+1}(\tau) - \theta_{n-1}(\tau)]\right\}, \tag{8}$$

which we refer to as the phase diffusion equation. The parameter ϵ_n provides a measure of fabricational imperfection, being defined as

$$\epsilon_n = 2\left(\frac{F_n - B_n}{F_n + B_n}\right). \tag{9}$$

Equation (8) is derived in Appendix A subject to the assumption that

$$\frac{1}{2}\epsilon_n \tan \frac{1}{2}[\theta_{n+1}(\tau) - \theta_{n-1}(\tau)] \ll 1. \tag{10}$$

Thus, Eq. (8) is only approximately correct when $\epsilon_n \neq 0$; however, the simpler, less general equation that results when $\epsilon_n = 0$ is exactly equivalent to Eq. (4) when $F_n = B_n$.

EQUILIBRIUM PHASE DISTRIBUTIONS

Analysis

Equilibrium solutions of Eq. (8) are obtained by recognizing that

$$\lim_{\tau\to\infty} \theta_n(\tau + 1) = \lim_{\tau\to\infty} \theta_n(\tau) \equiv \theta_n, \tag{11}$$

the final equality being a convenient notational convention. With the additional definition

$$\Delta\theta_n \equiv \theta_n - \theta_{n-1}, \tag{12}$$

it follows from Eqs. (8) and (11) that in the infinite-time limit

$$\Delta\theta_{n+1} = \Delta\theta_n + \epsilon_n \tan \frac{1}{2}(\Delta\theta_{n+1} + \Delta\theta_n). \tag{13}$$

If we are to have a uniform phase gradient,

$$\Delta\theta_n = \Delta\theta_{n+1} = \text{constant}, \tag{14}$$

it follows from Eqs. (9) and (13) that we must have equal forward and backward coupling,

$$F_n = B_n, \tag{15}$$

i.e., $\epsilon_n = 0$. Feed networks for which Eq. (15) obtains are referred to as "fabricationally perfect." If $F_n \neq B_n$, i.e., if $\epsilon_n \neq 0$, for one or more values of n, the network is referred to as "fabricationally imperfect."

From Eqs. (5) and (12),

$$\sum_{m=1}^{n} \Delta\theta_m = (\theta_n - \theta_0) = \theta_n, \tag{16}$$

and

$$\sum_{m=1}^{M} \Delta\theta_m = (\theta_M - \theta_0) = M\Delta\phi - s \cdot 2\pi, \tag{17}$$

where s is an integer. The term $s \cdot 2\pi$ appearing in Eq. (17) reflects the fact that the phase difference $(\theta_M - \theta_0)$ established by the phase shifter (cf. Fig. 2) is physically determinate only to within an integer multiple of 2π.

From Eq. (14),

$$\sum_{m=1}^{n} \Delta\theta_m = n\Delta\theta_n\,, \quad n = 1,\ 2,\ \ldots\ M. \tag{18}$$

The equilibrium phase distribution for fabricationally perfect CAM networks follows from Eqs. (16), (17), and (18).

$$\left.\begin{aligned} \Delta\theta_n(\infty) &= \Delta\phi - (s \cdot 2\pi/M) \\ \theta_n(\infty) &= n\Delta\theta_n(\infty) \end{aligned}\right\} \quad n = 1,\ 2,\ \ldots\ M, \tag{19}$$

where s is an integer.

To complete the specification of the physical problem, and to provide necessary information for calculating the indeterminate integer s appearing in Eq. (19), we must specify values for the initial phase distribution, Eq. (6). Assuming that the network is initially in an equilibrium state we may write

$$\theta_n(\tau) = \theta_n^i = n\Delta\phi_0\,, \quad n = 1,\ 2,\ \ldots\ M,\ \tau < 0. \tag{20}$$

For initial conditions and boundary conditions specified by Eqs. (20) and (5), respectively, it has been found by computer simulation that the only values of s ever to occur are $s = 0$ and $s = 1$.

Figure 5 shows the initial phase distribution, Eq. (20), and the two possible final phase distributions (Eq. (19) with $s = 0$ and $s = 1$). We now summarize some results from Appendix B addressing the question of which of these two final phase distributions is ultimately established.

For positively coupled lattices, $F > 0$,

$$s = \begin{cases} 0, & 0 \leqslant \alpha_M(0) < (\pi - 2\Delta\phi_0) \\ 1, & \text{otherwise.} \end{cases} \tag{21}$$

For negatively coupled modules, $F < 0$,

$$s = \begin{cases} 0, & 0 \leqslant \alpha_M(0) < (3\pi - 2\Delta\phi_0) \\ 1, & \text{otherwise.} \end{cases} \tag{22}$$

We recall that the quantity $\alpha_M(0)$ appearing in Eqs. (21) and (22) was defined in Eq. (7) as the step change in boundary phasing imposed by the phase-shifter at time $\tau = 0$.

To summarize, the equilibrium phase distribution θ_n (or $\Delta\theta_n$) is calculated subject to two assumptions:

- We assume that the network is initially in an equilibrium state characterized by the initial phase gradient $\Delta\theta_n(\tau) = \Delta\phi_0$, $\tau < 0$.
- We assume that the setting of the phase control in Fig. 2 is changed by an amount $\mathrm{mod}_{2\pi}(\theta_M^f - \theta_M^i) = \alpha_M(0)$, having a value between 0 and 2π.

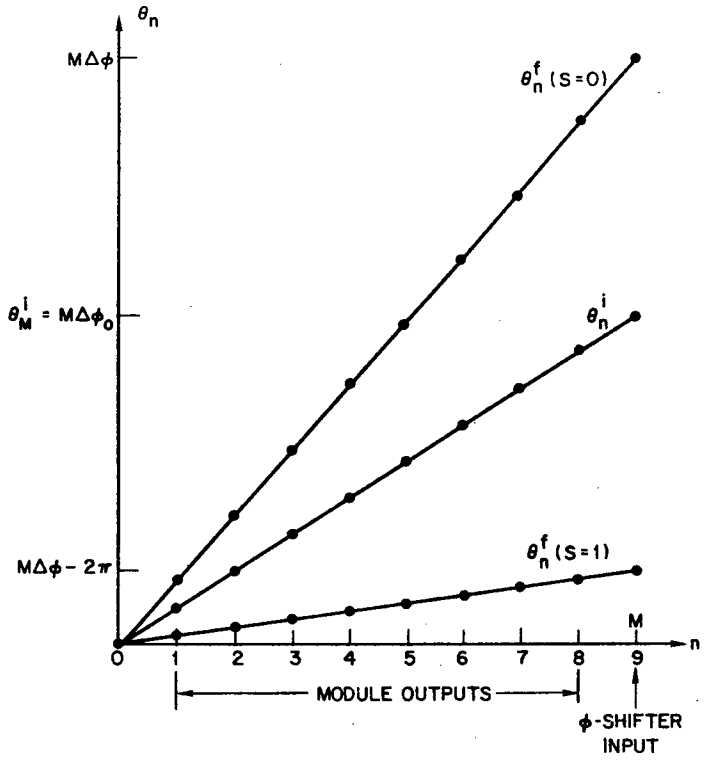

Fig. 5 — Phase distributions for an 8-module linear lattice ($M = 9$). The initial phase distribution θ_n^i has a phase gradient of $\Delta\phi_0$ per module. The initial distribution evolves into one of two possible final distributions, θ_n^f, referred to as the $s = 0$ and $s = 1$ equilibrium phase distributions. The $s = 0$ distribution is established if $0 < \mathrm{mod}_{2\pi}(\theta_M^f - \theta_M^i) < (\pi - 2\Delta\phi_0)$.

The network will settle into a new equilibrium phase distribution that can be calculated as follows.

- The value of s is computed from Eq. (21) if $F > 0$ or from Eq. (22) if $F < 0$.
- The quantity $\Delta\phi$ is computed from the equation

$$\Delta\phi = \Delta\phi_0 + [\alpha_M(0)/M]. \tag{23}$$

  Since $\alpha_M(0)$ is always positive by definition (cf. Eq. (7)), Eq. (23) ensures that $\Delta\phi > \Delta\phi_0$, always.

- The values for $\Delta\phi$ and s are substituted into Eq. (19) to obtain the new equilibrium phase distribution.

Appendix B provides expanded discussion of the equilibrium phase distributions.

Phasing Limitations and an Alternative Module Structure

Inspection of Fig. 5 shows that development of the $s = 0$ phase distribution corresponds to the evolution of a larger phase gradient than existed initially,

$$\Delta\theta_n > \Delta\phi_0, \quad s = 0. \tag{24}$$

It follows from Eqs. (21) and (24) that

$$\alpha_M(0) < (\pi - 2\Delta\phi_0), \tag{25}$$

from which, together with Eqs. (19) and (7), we can show that

$$(\Delta\theta_n - \Delta\phi_0) < (\pi - 2\Delta\phi_0)/M. \tag{26}$$

Equation (26) indicates that the achievable increment in phase gradient becomes ever smaller as the initial gradient approaches 90° per module. Thus, *phase gradients* $|\Delta\theta_n| > 90°$ *per module are unattainable with positively coupled lattices* ($F > 0$). Similarly, we find that phase gradients $0 < |\Delta\theta_n| < 90°$ per module are unattainable for CAM lattices with negative coupling ($F < 0$). Appendix B provides a more detailed discussion of the phasing limitations.

One method of achieving full hemispheric scanning capability (up to ±180° phase differential between antenna elements) is to allocate two modules per radiating element (cf. Fig. 2). Alternatively, only one module per antenna need be used if the module is designed as shown in Fig. 6. As compared with the original Fig. 3 module, the Fig. 6 module incorporates a 180° 1-bit phase-shifter. The modified CAM network is made to simulate the original network for small phase gradients, $0 \leqslant \Delta\phi < 90°$ per module, by setting all 1-bit phase-shifters to their 0°-state. Scanning at large angles, requiring $90° < \Delta\theta_n < 180°$ per module, is achieved by setting all 1-bit phase-shifters to their 180°-state (corresponding to negative coupling, $F < 0$). Thus, utilizing the Fig. 6 module rather than the Fig. 3 module we may replace all nonradiating terminations in Fig. 2 with radiating elements and still retain full hemispheric scan. Of course, the expense saved in halving the number of modules may be more than completely offset by the increased cost per module.

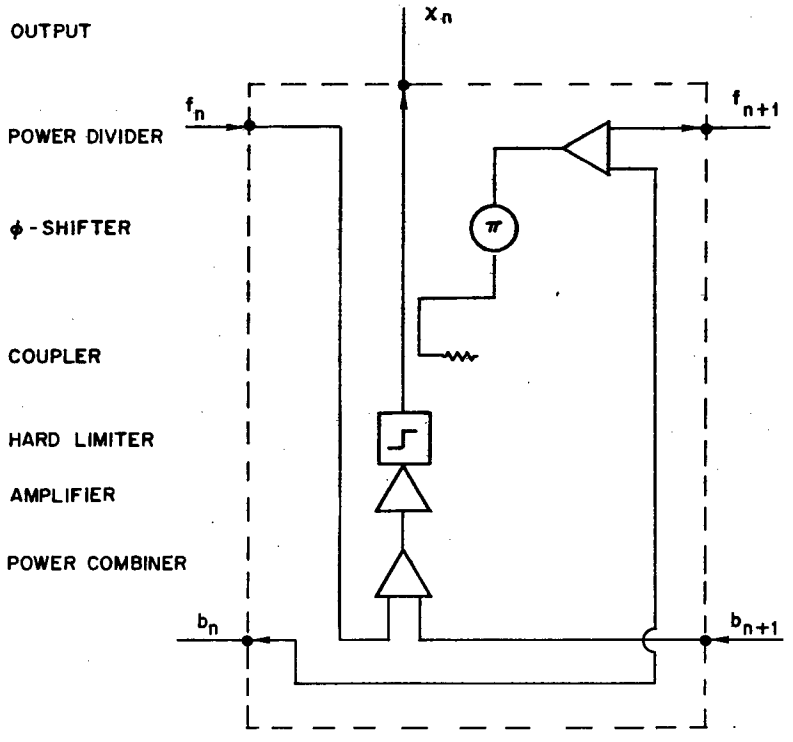

Fig. 6 — Amplifier/limiter module incorporating 1-bit 180° phase-shifter, permitting full hemispheric scan with just one module per radiating element

TRANSIENT PHASE DISTRIBUTION AND SETTLING TIME

We presently assume that the CAM lattice is fabricationally perfect, i.e., that Eq. (15) obtains for all values of n. It follows from Eqs. (8), (9), and (15) that

$$\theta_n(\tau + 1) = \frac{1}{2}[\theta_{n+1}(\tau) + \theta_{n-1}(\tau)]. \tag{27}$$

Equation (27) is solved in Appendix C by the separation of variables method. The exact solution is

$$\theta_n(\tau) = \theta_n(\infty) + 2[\Delta\theta_n(\infty) - \Delta\phi_0] \sum_{k=1}^{[M/2]} (-1)^k \left[\frac{\sin(nk\pi/M)}{\sin(k\pi/M)}\right] [\cos(k\pi/M)]^{\tau+\mu}, \tag{28}$$

where $[M/2]$ denotes the integer part of $(M/2)$, quantity $\Delta\theta_n(\infty)$ is the equilibrium phase distribution, Eq. (19), and

$$\mu \equiv \frac{1}{2}[1 + (-1)^{n+\tau+M}] = \begin{cases} 0, & (n + \tau + M) \text{ odd} \\ 1, & (n + \tau + M) \text{ even.} \end{cases} \tag{29}$$

The factor $[\Delta\theta_n(\infty) - \Delta\phi_0]$ appearing in Eq. (28) may be calculated from Eqs. (19) and (23) as

$$[\Delta\theta_n(\infty) - \Delta\phi_0] = [\alpha_M(0) - s2\pi]/M, \tag{30}$$

where $\alpha_M(0)$ is the step-change in edge phasing, as defined by Eq. (7), and s is given by Eq. (21) if $F > 0$ or Eq. (22) if $F < 0$.

Values of $\theta_n(\tau)$ calculated from Eq. (28) have been compared with the results of iterative numerical solutions of Eq. (4). The exact equality of θ_n values calculated by these two totally different methods is taken as a validation of Eq. (28).

In the limit $(k\pi/M) << 1$, valid for small k,

$$[\cos(k\pi/M)]^{\tau} \simeq e^{-\tau/\tau_k}, \tag{31}$$

where the time constants τ_k are given by

$$\tau_k \simeq \frac{1}{5}(M/k)^2. \tag{32}$$

It follows from Eqs. (31) and (32) that the $k \geqslant 2$ terms in Eq. (28) decay much more rapidly with time than does the $k = 1$ term. Thus, we expect the long-time behavior of the phase distribution to be dominated by the $k = 1$ term,

$$\hat{\theta}_n(\tau) = \theta_n(\infty) - 2[\Delta\theta_n(\infty) - \Delta\phi_0]\left[\frac{\sin(n\pi/M)}{\sin(\pi/M)}\right] e^{-(\tau+\mu)/\tau_s}, \tag{33}$$

where μ is again given by Eq. (29), and the settling time τ_s is defined as

$$\tau_s \equiv \tau_1 = M^2/5. \tag{34}$$

A simple single-mode approximation also may be obtained for the phase gradient $\Delta\theta_n$, Eq. (12),

$$\Delta\hat{\theta}_n(\tau) = \Delta\theta_n(\infty) - 2[\Delta\theta_n(\infty) - \Delta\phi_0] \cos[(n + \mu - 1)\pi/M] e^{-\tau/\tau_s}. \tag{35}$$

The single mode approximations, Eq. (33) and (35), are highly accurate for

$$\tau > \tau_s.$$

We have compared the approximate solution, Eq. (35), with the complete analytic solution obtained from Eq. (28) and with iterative computer solutions of Eq. (4). The sample calculations presented below assume that

$$(M,\ \Delta\phi_0,\ \alpha_M(0)) = (9,\ 60°,\ 45°). \tag{36}$$

That is, we assume an 8-module feed initially in an equilibrium state described by Eq. (20) with a uniform phase gradient of 60° per module. We further assume that the equilibrium prevailing for $\tau < 0$ is disturbed at $\tau = 0$ by step-increasing the phase control in Fig. 2 by $\alpha_9(0) = 45°$. We find from Eqs. (21) and (23) that the network will eventually settle into a new equilibrium phase distribution given by Eq. (19) with

$$\Delta\theta_n(\infty) = \Delta\phi = 65°. \tag{37}$$

For this calculation (and all other calculations) the numerical solution was in exact agreement with Eq. (28).

Figure 7 shows the phase distribution as a function of module index n at two values of time ($\tau = 32$ and $\tau = 48$), for the specified parameter values, Eq. (36). Approximation $\Delta\hat{\theta}_n$ is indistinguishable from the exact solution on the scale of Fig. 7.

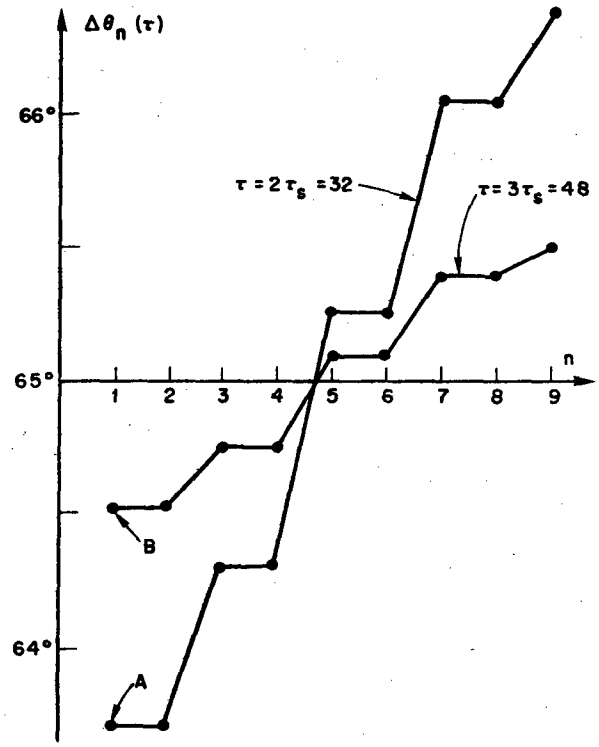

Fig. 7 — Phase distribution for an 8-module feed at two values of time ($\tau = 32$ and $\tau = 48$). Assumed parameter values were $(M,\ \Delta\phi_0,\ \alpha_M(0)) = (9,\ 60°,\ 45°)$. In the infinite-time limit a uniform phase gradient is established, $\Delta\theta_n(\infty) = \Delta\phi = 65°$.

Figure 8 depicts the transient development of $\Delta\theta_1(\tau)$ obtained by the exact methods of solution. Figure 9 shows the difference between the exact and approximate solutions for $\Delta\theta_1(\tau)$ as a function of time. We see from Fig. 9 that the error incurred in using Eq. (35), rather than the complete solution, is less than 0.13° for $\tau > \tau_s = 16$.

MODULES WITH FABRICATIONAL IMPERFECTIONS

Approximate Formulation for the Equilibrium Phase Distribution

Up to this point in our analysis we assume that all components in the CAM network, Fig. 2, can be fabricated to arbitrarily precise specifications. In particular, we assume that the power splitters have been fabricated to achieve perfectly equal forward and backward coupling, Eq. (15). It is of some interest to quantify how component imperfections degrade the phasing accuracy of the CAM network.

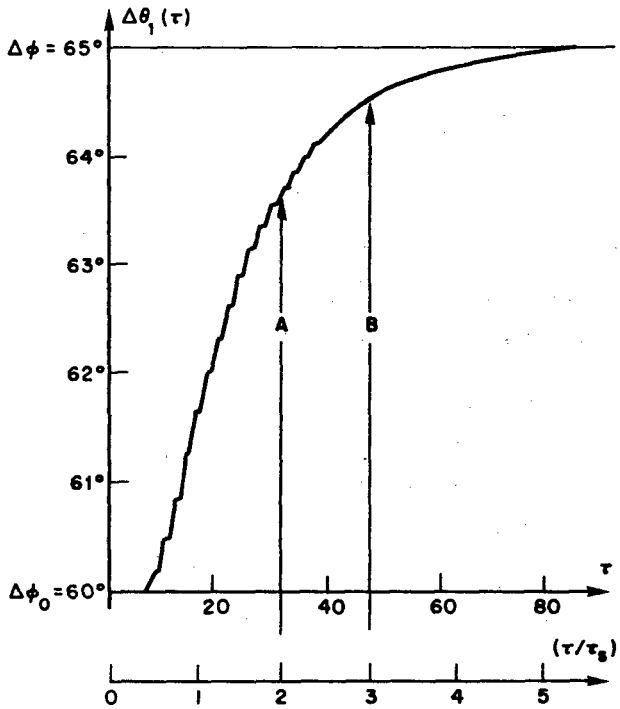

Fig. 8 — Transient development of $\Delta\theta_1(\tau)$ for the same parameter values as Fig. 7. Values at $\tau = 2\tau_s$ (point A) and $\tau = 3\tau_s$ (point B) correspond to points A and B in Fig. 7. Values given can be obtained from either of the two exact methods of solution: the complete analytical solution, Eq. (28), or by numerical solution of Eq. (4).

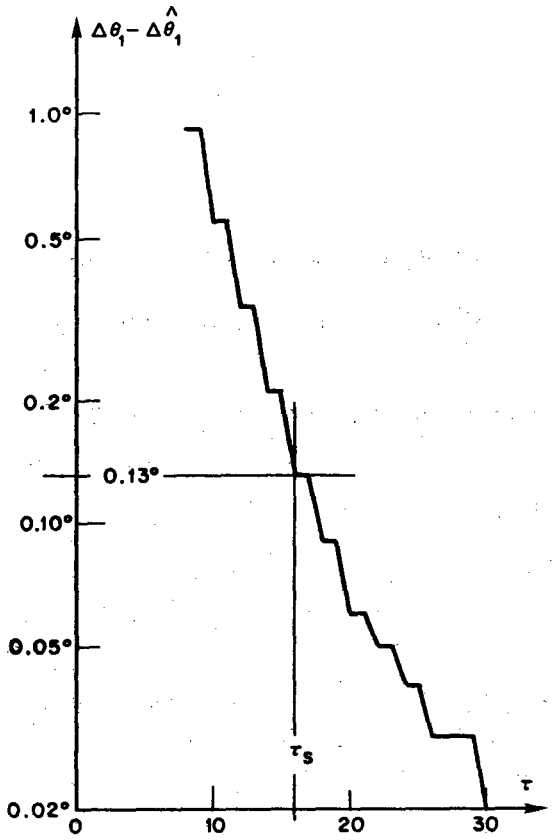

Fig. 9 — Values plotted are the difference between the exact value of $\Delta\theta_1$ (Fig. 8) and the approximate value $\Delta\hat{\theta}_1$ obtained from Eq. (35). Error incurred in using $\Delta\hat{\theta}_1$ is less than 0.13° for $\tau > \tau_s$.

We presently relax Eq. (15) somewhat, assuming instead that

$$0 < |\epsilon_n| << 1, \tag{38}$$

for at least one value of n (cf. Eq. (9)). Our interest is in obtaining the solution of Eq. (13). We have shown previously that when $\epsilon_n = 0$, $n = 1, 2, \ldots (M-1)$, the equilibrium phase distribution is a uniform phase gradient, as desired,

$$\Delta\theta_n^0(\infty) = \Delta\phi_0 + [\alpha_M(0) - s \cdot 2\pi]/M, \tag{39}$$

or, equivalently,

$$\Delta\theta_n^0(\infty) = \Delta\phi - s(2\pi/M). \tag{40}$$

The superscript 0 on $\Delta\theta_n^0(\infty)$ serves as a reminder that Eqs. (39) and (40) are derived subject to the assumption that $\epsilon_n = 0$. We now define a new quantity $\Delta\phi_n$ that measures the degree to which the actual phase gradient $\Delta\theta_n$ departs from the ideal, i.e.,

$$\Delta\phi_n = \Delta\theta_n(\infty) - \Delta\theta_n^0(\infty), \tag{41}$$

with $\Delta\theta_n^0(\infty)$ given by Eq. (39).

Appendix D shows that Eq. (13) has the approximate solution

$$\Delta\phi_n \cong \left\{ \frac{1}{M} \sum_{r=1}^{M} \sum_{p=r}^{M} \epsilon_p - \sum_{p=n}^{M} \epsilon_p \right\} \tan \Delta\theta_n^0(\infty), \quad n = 1, 2, \ldots M. \tag{42}$$

In the remainder of this section we assume that $s = 0$, allowing us to replace $\Delta\theta_n^0(\infty)$ by $\Delta\phi$ in Eq. (42).

Feeds with Identical Imperfect Modules

If all the modules in the CAM network are identical, even though they are imperfect, we have

$$\epsilon_n = \epsilon, \tag{43}$$

independent of the module index n. Subject to Eq. (43), Eq. (42) becomes (cf. Eq. (D26))

$$\Delta\phi_n \cong \epsilon[n - (M + 1)/2] \tan \Delta\phi, \quad n = 1, 2, \ldots M, \tag{44}$$

where

$$\epsilon = 2(F - B)/(F + B).$$

In Fig. 10 we present values predicted by a computer solution of Eq. (4), for the parameter values

$$(\epsilon, \Delta\phi, M) = (10^{-2}, 65°, 9). \tag{45}$$

We observe from Fig. 11 that Eq. (44) agrees fairly well with the numerical solution. In Appendix D we calculate a second-order correction to Eq. (44) that results in an even closer fit to the numerical solution.

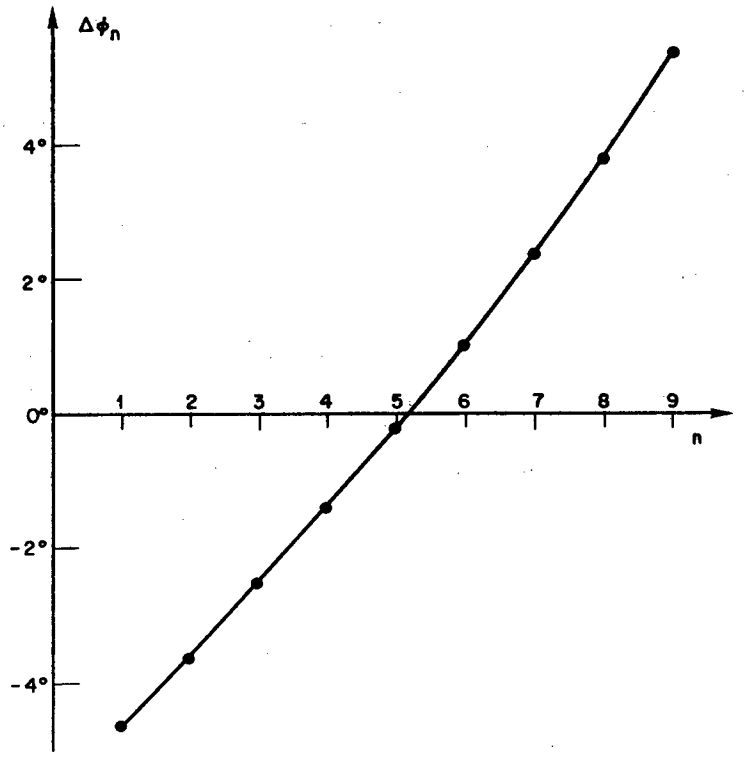

Fig. 10 — Equilibrium phase error for an 8-module feed with identical imperfect modules, obtained by numerical solution of Eq. (4). Parameter values assumed are $(\epsilon, \Delta\phi, M) = (0.01, 65°, 9)$.

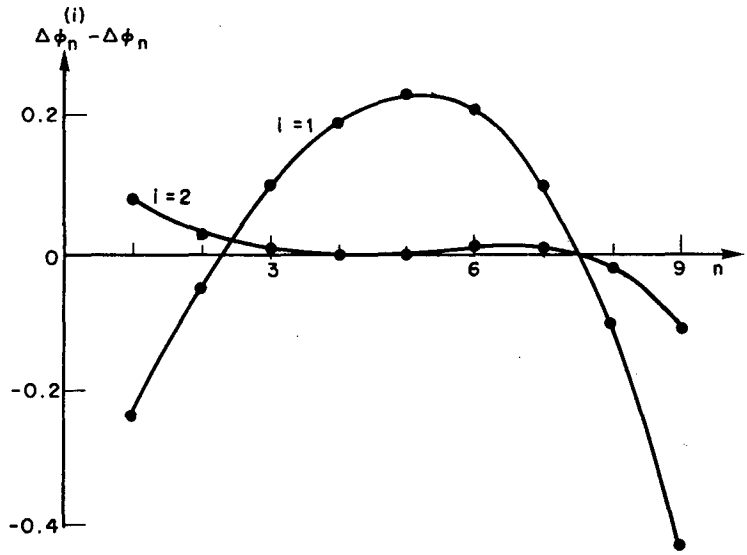

Fig. 11 — Difference between exact value of $\Delta\phi_n$, as given in Fig. 10, and value of $\Delta\phi_n$ obtained by two approximate formulations. The first-order approximation $\Delta\phi_n^{(1)}$ is given by Eq. (44); the second-order approximation $\Delta\phi_n^{(2)}$ is given by Eq. (D41).

We note from Fig. 10 that the phase increment per module $\Delta\theta_n$ varies from a minimum of

$$\Delta\theta_1 = (\Delta\phi_1 + \Delta\phi) \simeq 60°,$$

to a maximum of

$$\Delta\theta_M = (\Delta\phi_M + \Delta\phi) \simeq 70°,$$

across the network. Thus, a systematic imperfection of 1% in the power split ratio gives rise to a phase inaccuracy of $\pm 5°$. However, smaller phase errors are obtained for smaller phase gradients, $\Delta\phi < 65°$, due to the tan $\Delta\phi$ factor in Eq. (44).

Defining a mean-square phase error as

$$\Delta\phi_{\text{rms}}^2 = \frac{1}{M}\sum_{n=1}^{M}(\Delta\phi_n)^2, \tag{46}$$

it follows from Eq. (44) that (in radians)

$$\Delta\phi_{\text{rms}} = \epsilon \tan\Delta\phi \left(\frac{1}{12}\right)^{1/2} M. \tag{47}$$

For our previous example, Eq. (45), we calculate

$$\Delta\phi_{\text{rms}} = 3.2°. \tag{48}$$

Random Imperfections

Rather than take ϵ_n as a known function of n (e.g., Eq. (43)) we now assume that the coupling coefficients F_n and B_n are independent, identically distributed random variables. The quantities ϵ_n are thus also independent and identically distributed,

$$E\{\epsilon_p\epsilon_k\} = \begin{cases}\sigma_\epsilon^2, & p = k \\ 0, & p \neq k,\end{cases} \tag{49}$$

where $E\{\cdot\}$ is the statistical expectation operator.

We show in Appendix E that the following approximate relationship obtains between the statistics of ϵ and those of F,

$$\sigma_\epsilon = \sqrt{2} \times 10^{-2} A, \tag{50}$$

where A is the percentage fabricational error,

$$A = 100(\sigma_F/\mu_F). \tag{51}$$

The quantity σ_ϵ in Eq. (50) is the standard deviation of ϵ_n; quantities σ_F and μ_F in Eq. (51) are the standard deviation of F_n and the mean value of F_n, respectively.

The variance of the phase error is defined as

$$\sigma_n^2 \equiv E(\Delta\phi_n^2) - [E(\Delta\phi_n)]^2. \tag{52}$$

It is shown in Appendix D from Eqs. (42), (49), and (52) that (in radians)

$$\sigma_n \simeq \sigma_\epsilon \tan \Delta\phi \left(\frac{1}{12}\right)^{1/2} M^{1/2}\{1 + 12M^{-2}[n - (M+1)/2]^2\}^{1/2}. \tag{53}$$

Equation (53) displays the expected symmetry about $n = (M+1)/2$. The minimum value of σ_n is obtained at the center of the array; from Eq. (53)

$$\sigma_{\min} = \min_n \sigma_n \simeq \sigma_\epsilon \tan \Delta\phi \left(\frac{1}{12}\right)^{1/2} M^{1/2}. \tag{54}$$

Equation (54) bears an interesting resemblance to Eq. (47); however, it should be remembered that $\Delta\phi_{\text{rms}}$ was defined on the basis of a spatial average, Eq. (46), while the values of σ_n, $n = 1, 2, \ldots M$, are established as ensemble coverages over the statistics of F_n.

From Eqs. (50), (51) and (53) we obtain (in degrees)

$$\sigma_n = 0.234\, A \tan \Delta\phi\, M^{1/2} \left\{1 + 12M^{-2}[n - (M+1)/2]^2\right\}^{1/2}, \quad n = 1, 2, \ldots M. \tag{55}$$

We find from Eq. (55) that the RMS phase error is minimum at the center of the array,

$$\sigma_{\min} = 0.234\, A \tan \Delta\phi\, M^{1/2}, \quad \text{degrees}, \tag{56}$$

and maximum at the edges of the array

$$\sigma_{\max} \simeq 2(1 - 0.75M^{-1})\sigma_{\min}. \tag{57}$$

We find from Eqs. (56) and (57) that when

$$(A, M, \Delta\phi) = (1\%, 9, 45°),$$

the minimum and maximum RMS phase errors are

$$\sigma_{\min} = \sigma_5 = 0.70°,$$

and

$$\sigma_{\max} = \sigma_1 = \sigma_9 = 1.29°.$$

Thus, a 1% RMS error in the power splits gives rise to about a 1° RMS phase gradient error.

MODULES WITH SELF-COUPLING

Our analysis thus far assumes that the coupled module lattice comprises of amplifier/limiter modules each configured as shown in Fig. 3. However, alternative module structures are conceivable, such as that depicted in Fig. 12. Comparison of Fig. 12 with Fig. 3 shows that the only difference between the two structures is the presence of a self-coupling path in Fig. 12.

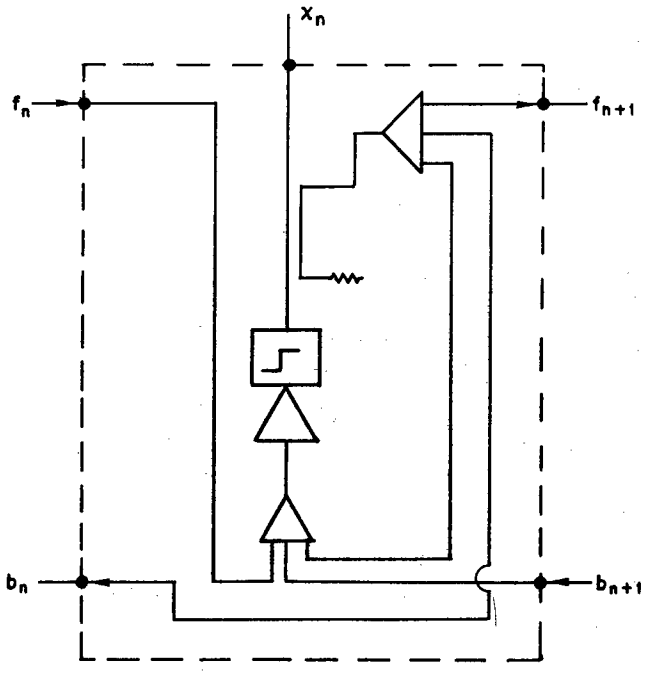

Fig. 12 — Amplifier/limiter module with self-coupling

A transient analysis of CAM lattices composed of self-coupled modules is given in Appendix F. It turns out that the self-coupled module, Fig. 12, has less desirable performance characteristics than the simpler module analyzed previously.

In brief, we find in Appendix F that (cf. Eq. (F34))

$$[\Delta\theta_n(\tau) - \Delta\theta_n(\infty)] \alpha e^{-\tau/T_s} \tag{58}$$

for self-coupled modules, Fig. 12. The settling time T_s in Eq. (58) is given by

$$T_s = \tau_s \left[1 + \frac{1}{2} F^{-1} \sec \Delta\phi\right], \tag{59}$$

where $\tau_s = M^2/5$ is the settling time for modules without self-coupling, Eq. (34). Stable equilibrium phase distributions exist only for $0 \leqslant \Delta\phi < \pi/2$ when $F > 0$; stable distributions exist only for $\pi/2 \leqslant \Delta\phi < \pi$ when $F < 0$. It follows from Eq. (59) that

$$T_s \geqslant \tau_s, \tag{60}$$

always, i.e., modules without self-coupling settle faster than modules with self-coupling.

Figure 13 depicts the transient development of $\Delta\theta_1(\tau)$ obtained by means of the theory developed in Appendix F, for the same parameter values as Figs. 7 and 8. Comparison between Figs. 13 and 8 shows that the phase distribution for self-coupled modules evolves more slowly with time and is temporally smoother than the phase distribution of modules that lack self-coupling.

According to Eq. (59),

- settling is faster for strong coupling (large F) than for weak coupling (small F). However, settling time cannot be decreased indefinitely by increasing F; once $F \cos \Delta\phi >> 1$ further increases in F provide no further improvement. We find that

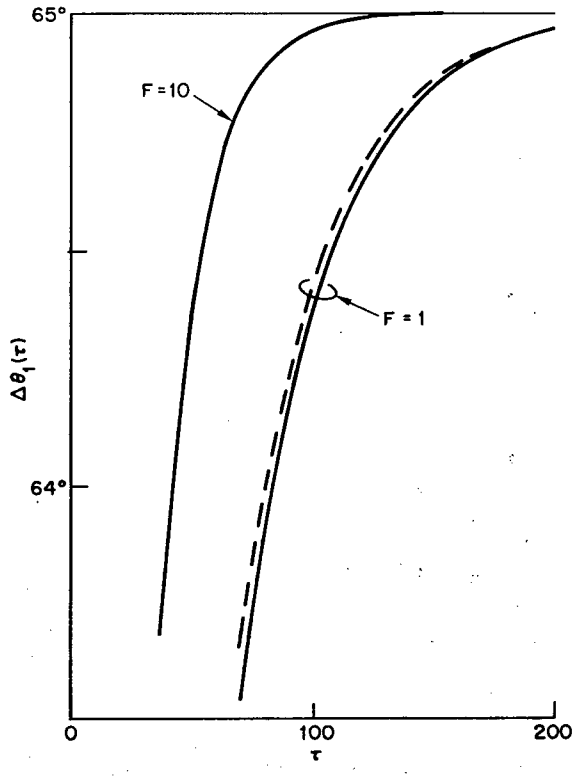

Fig. 13 — Transient development of $\Delta\theta_1(\tau)$ for a self-coupled CAM lattice. Assumed parameter values are $(M, \Delta\phi_0, \alpha_M(0)) = (9, 60°, 45°)$, for all curves. Strong coupling, $F = 10$, results in faster settling than unity coupling, $F = 1$. Solid curves obtained by numerical solution of Eq. (F1); dashed curves obtained by one-mode approximation, Eq. (F34). Solid and dashed curves for $F = 10$ are too close to distinguish on this plot.

$$\lim_{F\to\infty} T_s = \tau_s, \tag{61}$$

i.e., we can do no better than the settling time obtainable by eliminating the self-coupling. Also,

- settling time becomes progressively longer, approaching infinity, as $\Delta\phi$ approaches 90°.

The longer settling time, Eq. (60), and the dependence of settling time on phasing, Eq. (59), are undesirable attributes that lead us to favor modules without self-coupling over modules with self-coupling.

TWO-DIMENSIONAL ARRAYS

We now briefly discuss how our results for 1-D CAM lattices can be extended to 2-D structures, appropriate as feeds for 2-D phased arrays.

We adopt an abbreviated convention for depicting CAM lattices, as illustrated in Fig. 14 for the previously analyzed 1-D structure. The empty circles in Fig. 14 denote amplifier/limiter modules terminated by antennas; filled circles denote modules with nonradiating terminations. Thus, Fig. 14 is equivalent to Fig. 2.

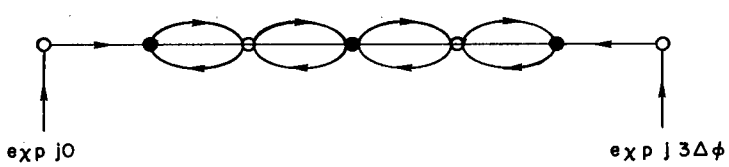

Fig. 14 — One-dimensional CAM lattice. Empty circles denote amplifier/limiter modules terminated by an antenna; filled circles denote modules with nonradiating terminations. This figure is equivalent to Fig. 2.

Figure 15 is a 2-D generalization of Fig. 14. Based on results already given, it is easily shown that the equilibrium phase distribution of the Fig. 15 lattice is the desired 2-D linear phase gradient. We can see by inspection that the settling time for the 2-D square lattice must satisfy the constraint

$$\tau_s(1\text{-}D) < \tau_s(2\text{-}D) < 2\tau_s(1\text{-}D),$$

where

τ_s (1-D) = $M^2/5$ is the settling time of 1-D edge lattice,

and

τ_s (2-D) is the settling time of 2-D lattice.

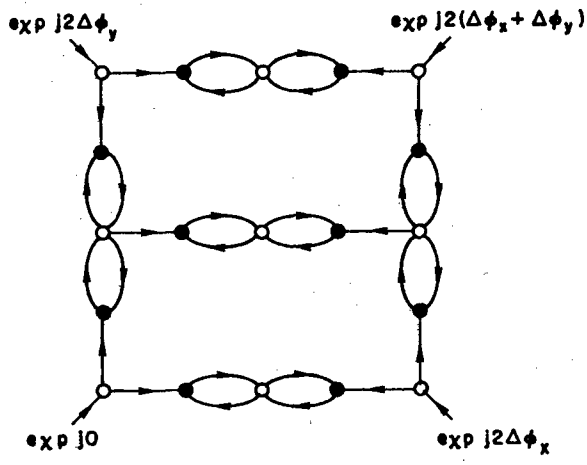

Fig. 15 — Two-dimensional CAM lattice suitable for exciting a 2-D phased-array. While only three phase-shifters are required to excite a rectangular structure of arbitrary size, settling time increases as the square of the largest linear dimension of the lattice. Thus, additional phase-shifters may be required to satisfy bandwidth requirements.

ACKNOWLEDGMENTS

The coupled amplifier module technique was originally conceived by Mr. J. Paul Shelton, Naval Research Laboratory, Washington, D.C. The author gratefully acknowledges technical discussions with Mr. Shelton during the course of this research. Special thanks are also due to Dr. James K. Hsiao, Naval Research Laboratory, for making available his CAM lattice computer simulation program.

REFERENCES

1. N. Goto and D. K. Cheng, "Phase-Shifter Thinning and Sidelobe Reduction for Large Phased Arrays," IEEE Trans. Antennas Propag. **AP-24** (2): 139-143, March 1976.

2. L. Stark, "Microwave Theory of Phased-Array Antennas—A Review," Proc. IEEE **62**, (12): 1661-1701, December 1974.

3. P. L. Meyer, *Introductory Probability and Statistical Applications*, Second Edition (Addison-Wesley, Reading, Mass., 1970).

Appendix A
THE PHASE DIFFUSION EQUATION

Taking the imaginary part of Eq. (4) we obtain

$$\sin \theta_n(\tau + 1) = N_n(\tau) \cdot S_n(\tau), \tag{A1}$$

where, by definition,

$$S_n(\tau) = B_n \sin \theta_{n+1}(\tau) + F_n \sin \theta_{n-1}(\tau). \tag{A2}$$

Equation (A2) may be rearranged to obtain,

$$S_n(\tau) = \frac{1}{2}(B_n + F_n)(\sin \theta_{n+1} + \sin \theta_{n-1}) + \frac{1}{2}(B_n - F_n)(\sin \theta_{n+1} - \sin \theta_{n-1}). \tag{A3}$$

Applying some standard trigonometric identities to Eq. (A3),

$$S_n(\tau) = \cos \frac{1}{2}(\theta_{n+1}+\theta_{n-1}) \cos \frac{1}{2}(\theta_{n+1}-\theta_{n-1})$$
$$\{(B_n + F_n) \tan \frac{1}{2}(\theta_{n+1} + \theta_{n-1}) + (B_n - F_n) \tan \frac{1}{2}(\theta_{n+1} - \theta_{n-1})\}. \tag{A4}$$

Similarly, taking the real part of Eq. (4) we obtain

$$\cos \theta_n(\tau + 1) = N_n(\tau) \cdot C_n(\tau), \tag{A5}$$

where, by definition,

$$C_n(\tau) = B_n \cos \theta_{n+1}(\tau) + F_n \cos \theta_{n-1}(\tau). \tag{A6}$$

Equation (A6) can be recast as

$$C_n(\tau) = \cos \frac{1}{2}(\theta_{n+1} + \theta_{n-1}) \cos \frac{1}{2}(\theta_{n+1} - \theta_{n-1})$$
$$\{(B_n + F_n) - (B_n - F_n) \tan \frac{1}{2}(\theta_{n+1} + \theta_{n-1}) \tan \frac{1}{2}(\theta_{n+1} - \theta_{n-1})\}. \tag{A7}$$

Dividing Eq. (A1) by Eq. (A5), and substituting Eqs. (A4) and (A7) for $S_n(\tau)$ and $C_n(\tau)$,

$$\tan \theta_n(\tau + 1) = \left\{ \frac{\tan \frac{1}{2}(\theta_{n+1} + \theta_{n-1}) - \frac{1}{2} \epsilon_n \tan \frac{1}{2}(\theta_{n+1} - \theta_{n-1})}{1 + \frac{1}{2} \epsilon_n \tan \frac{1}{2}(\theta_{n+1} - \theta_{n-1}) \tan \frac{1}{2}(\theta_{n+1} + \theta_{n-1})} \right\}, \tag{A8}$$

where

$$\epsilon_n \equiv 2 \left[\frac{F_n - B_n}{F_n + B_n} \right]. \tag{A9}$$

We see immediately from Eq. (A8) that, for $F_n = B_n$,

$$\theta_n(\tau + 1) = \frac{1}{2}[\theta_{n+1}(\tau) + \theta_{n-1}(\tau)], \quad \epsilon_n = 0. \tag{A10}$$

Subtracting $\theta_n(\tau)$ from each side of Eq. (A10),

$$[\theta_n(\tau + 1) - \theta_n(\tau)] = \frac{1}{2}[\theta_{n+1}(\tau) - 2\theta_n(\tau) + \theta_{n-1}(\tau)]. \tag{A11}$$

Equation (A11) has the form of a one-dimensional heat flow equation in which the time and space derivatives have been replaced by finite differences. We refer to Eq. (A11) as the phase diffusion equation for perfect modules, i.e., modules for which $\epsilon_n = 0$.

More generally, further simplification of Eq. (A8) when $\epsilon_n \neq 0$ requires that we assume

$$\frac{1}{2}\epsilon_n \tan \frac{1}{2}(\theta_{n+1} - \theta_{n-1}) \ll 1, \tag{A12}$$

so that

$$\frac{1}{2}\epsilon_n \tan \frac{1}{2}(\theta_{n+1} - \theta_{n-1}) \simeq \tan\left\{\frac{1}{2}\epsilon_n \tan \frac{1}{2}(\theta_{n+1} - \theta_{n-1})\right\}. \tag{A13}$$

It follows from Eqs. (A8), (A13), and the trigonometric equality

$$\tan (A - B) = \frac{\tan A - \tan B}{1 + \tan A \tan B},$$

that

$$\theta_n(\tau + 1) = \frac{1}{2}\left\{\theta_{n+1}(\tau) + \theta_{n-1}(\tau) - \epsilon_n \tan \frac{1}{2}[\theta_{n+1}(\tau) - \theta_{n-1}(\tau)]\right\}. \tag{A14}$$

We refer to Eq. (A14) as the general phase diffusion equation.

Appendix B
EQUILIBRIUM PHASE DISTRIBUTIONS

ANALYSIS

For a given initial phase distribution, Eq. (20), and a specified step-increase in the boundary phasing at $\tau = 0$

$$\alpha_M(0) \equiv \mathrm{mod}_{2\pi}(\theta_M^f - \theta_M^i), \tag{B1}$$

the CAM network may evolve either of two possible phase distributions (cf. Fig. 5). We presently address the question of which of these two final phase distributions is ultimately established.

We have found by computer simulation that the parameter s in our analytically derived equilibrium phase distribution, Eq. (19), can be determined by inspecting the phase distribution after just a single delay time, $\tau = 1$. Only θ_{M-1}, one module removed from the point of disrupted excitation, has changed from its initial value at this time. Defining the time gradient of phasing as

$$\alpha_n(\tau) \equiv \mathrm{mod}_{2\pi}\{\theta_n(\tau) - \theta_n(\tau - 1)\}, \tag{B2}$$

we find that

$$\alpha_{M-1}(1) \equiv \mathrm{mod}_{2\pi}\{\theta_{M-1}(1) - \theta_{M-1}(0)\} \begin{cases} < \pi, & s = 0 \\ > \pi, & s = 1 \end{cases} \tag{B3}$$

The meaning of Eq. (B3) is interpreted with the aid of Figs. B1 and B2. Assuming that the phase distribution is given by Eq. (20) at time $\tau < 0$, we must determine whether $\theta_{M-1}(1)$ is greater or less than $\theta_{M-1}(0)$. First, we note that

$$\theta_n(0) = \theta_n(-1), \quad n = 0, 1, 2, \ldots (M-1), \tag{B4}$$

and

$$\theta_n(1) = \theta_n(0), \quad n = 0, 1, 2, \ldots (M-2), \tag{B5}$$

since the phase disturbance initiated at $(n, \tau) = (M, 0)$ propagates at the rate of one module per unit of normalized time. Comparing Fig. B1 and Fig. 5, we see that Fig. B1 corresponds to an incipient $s = 0$ phase distribution. Similarly, comparison with Fig. 5 shows that Fig. B2 corresponds to an incipient $s = 1$ distribution.

Setting $(n, \tau) = (M-1, 0)$ in Eq. (4) we obtain

$$e^{j\theta_{M-1}(1)} = N_{M-1}(0) F_{M-1}[e^{j\theta_M(0)} + e^{j\theta_{M-1}(0)}]. \tag{B6}$$

Multiplying both sides of Eq. (B6) by $\exp[-j\theta_{M-1}(0)]$ we obtain

$$e^{j\alpha_{M-1}(1)} = N_{M-1}(0) F_{M-1}[e^{j\Delta\theta_M(0)} + e^{-j\Delta\theta_{M-1}(0)}], \tag{B7}$$

where $\alpha_{M-1}(1)$ is defined by Eq. (B2) and the quantities $\Delta\theta_n(\tau)$ are defined by

$$\Delta\theta_n(\tau) \equiv \theta_n(\tau) - \theta_{n-1}(\tau). \tag{B8}$$

From Eqs. (B4) and (B8)

$$\Delta\theta_{M-1}(0) = \theta_{M-1}(-1) - \theta_{M-2}(-1). \tag{B9}$$

From Eqs. (B9) and (20),

$$\Delta\theta_{M-1}(0) = \Delta\phi_0. \tag{B10}$$

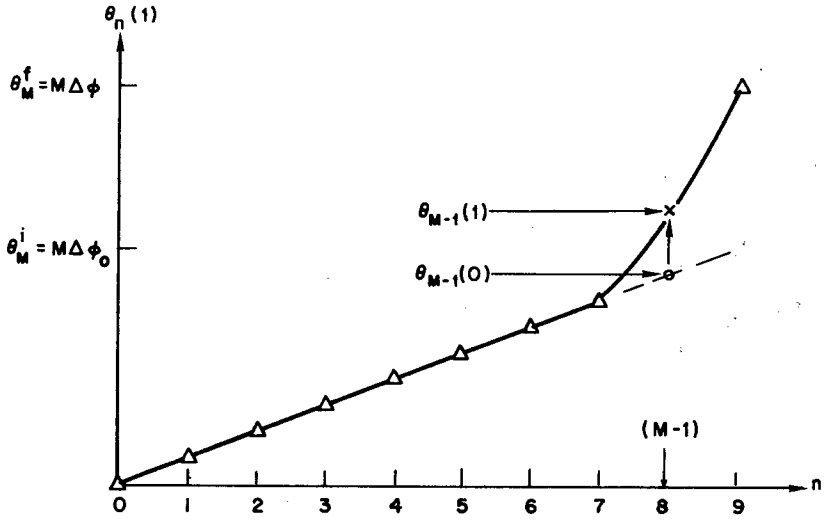

Fig. B1 — Incipient $S = 0$ equilibrium phase distribution. Circle (O) denotes value at $\tau = 0$. Cross (×) denotes value at $\tau = 1$. Triangle (Δ) denotes values that are the same at $\tau = 0$ and $\tau = 1$.

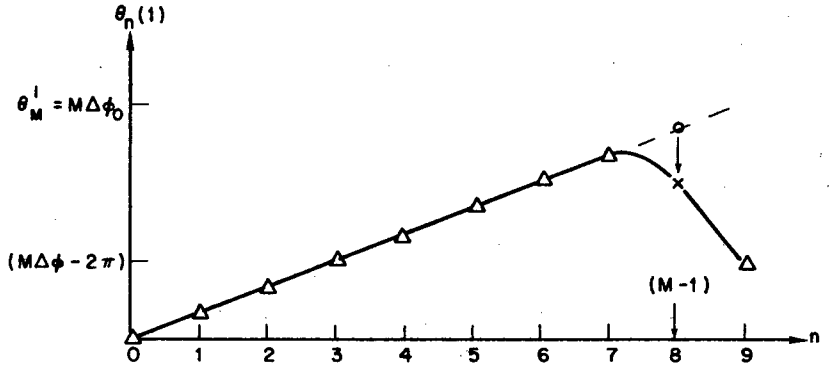

Fig. B2 — Incipient $S = 1$ equilibrium phase distribution.
Symbols O, ×, and Δ as in Fig. B1.

Similarly, we can show from Eqs. (5b), (B4), (B8), and (20) that

$$\Delta\theta_M(0) = \Delta\phi_0 + M(\Delta\phi - \Delta\phi_0). \tag{B11}$$

From Eqs. (B1) and (5b)

$$\alpha_M(0) = \mathrm{mod}_{2\pi}(\theta_M^f - \theta_M^i) = M(\Delta\phi - \Delta\phi_0). \tag{B12}$$

Substituting Eqs. (B10) and (B11) into Eq. (B7), and making use also of Eq. (B12), we obtain

$$e^{j\alpha_{M-1}(1)} = N_{M-1}(0)F_{M-1}[e^{j\Delta\phi_0}e^{j\alpha_M(0)} + e^{-j\Delta\phi_0}]. \tag{B13}$$

Equation (B13) is given a phasor diagram representation in Fig. B3, for positive coupling ($F_{M-1} > 0$).

We see from Fig. B3 that $\alpha_{M-1}(1) < \pi$ so long as

$$0 < \alpha_M(0) < (\pi - 2\Delta\phi_0). \tag{B14}$$

In interpreting Eq. (B14) we recall that $\alpha_M(0)$ is the change in edge phasing imposed by the phase-shifter, as given by Eq. (B12). If we do not increase the edge phasing by too large an amount, Eq.

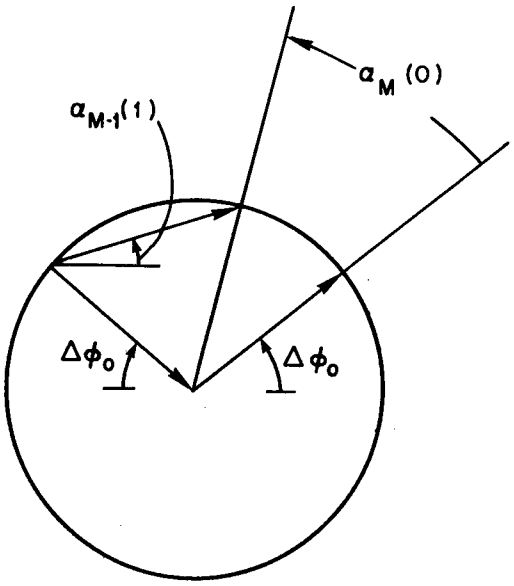

Fig. B3 — Phasor diagram derived from Eq. (B13), assuming $F > 0$. The $S = 0$ phase distribution (cf. Fig. 5) evolves when angle $\alpha_{M-1}(1) < \pi$, i.e., for $0 < \alpha_M(0) < (\pi - 2\Delta\phi_0)$.

(B14) will be satisfied and the $s = 0$ phase distribution will evolve after a period of time (cf. Fig. 5). However, if the edge phasing is increased to such an extent that Eq. (B14) is not satisfied, we find instead that the $s = 1$ phase distribution will ultimately evolve.

Figure B3 and the conclusions derived from it pertain to positive coupling ($F > 0$). The corresponding phasor diagram for negative coupling ($F < 0$), also derived from Eq. (B13), is shown in Fig. B4.

In general, the equilibrium phase distribution can be predicted from Eq. (19) and the following set of rules for assigning a value to the parameter s.

For positively coupled modules ($F > 0$; $0 \leqslant \Delta\phi_0 < \pi/2$),

$$s = \begin{cases} 0, & 0 \leqslant \alpha_M(0) < (\pi - 2\Delta\phi_0) \\ 1, & \text{otherwise.} \end{cases} \tag{B15}$$

For negative coupling ($F < 0$; $\pi/2 \leqslant \Delta\phi_0 < \pi$),

$$s = \begin{cases} 0, & 0 \leqslant \alpha_M(0) < (3\pi - 2\Delta\phi_0) \\ 1, & \text{otherwise.} \end{cases} \tag{B16}$$

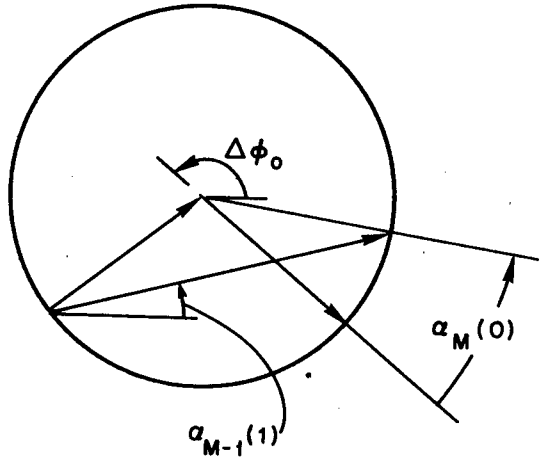

Fig. B4 — Phasor diagram derived from Eq. (B13), assuming $F < 0$. Note that $\Delta\phi_0 > 90°$. The $S = 0$ phase distribution (cf. Fig. 5) evolves when $\alpha_{M-1}(1) < \pi$, i.e., for $0 < \alpha_M(0) < (3\pi - 2\Delta\phi_0)$.

PHASING UP (s = 0 Phase Distributions)

By "phasing up" we mean the process of modifying the edge phasing to achieve a new equilibrium phase gradient that is larger than the initial gradient, $\Delta\theta_n > \Delta\phi_0$. Inspection of Fig. 5 shows that phasing up corresponds to the establishment of an $s = 0$ phase distribution.

From Eqs. (19), (21), and (23) (assuming $F > 0$),

$$\Delta\theta_n = \Delta\phi_0 + [\alpha_M(0)/M], \tag{B17a}$$

subject to the requirement that

$$0 \leqslant \alpha_M(0) < (\pi - 2\Delta\phi_0), \tag{B17b}$$

where $\Delta\phi_0$ is the initial phase gradient, $\Delta\theta_n$ is the new phase gradient, and $\alpha_M(0)$ is the step-change in edge phasing. According to Eq. (B17), the new phase gradient is proportional to the step-change in edge phasing, $\alpha_M(0)$, so long as $\alpha_M(0)$ is not too large. While Eq. (B17) is applicable only to positively coupled lattices ($F > 0$), an analogous formulation is readily derived for $F < 0$. The upper limit on $\Delta\theta_n$ established by Eq. (B17) is

$$\Delta\theta_n < [\Delta\phi_0 + (\pi - 2\Delta\phi_0)/M]. \tag{B18}$$

For example, we assume that

$$(\Delta\phi_0,\ M) = (60°,\ 9), \tag{B19}$$

i.e., that we have an 8-module feed initially phased to 60° per module. If we step-increase the edge phasing by just less than the upper limit indicated in Eq. (B17b), say,

$$\alpha_M(0) = 0.99(\pi - 2\Delta\phi_0) = 59.4°, \tag{B20}$$

the lattice will eventually settle into a new phase distribution

$$\Delta\theta_n = 60° + (59.4°/9) = 66.6°, \tag{B21}$$

just less than the upper limit established by Eq. (B18), $\Delta\theta_n < 66.67°$. If we attempt to increase $\Delta\theta_n$ above 66.67° by step-increasing θ_M by an amount $\alpha_M(0) > (\pi - 2\Delta\phi_0)$, the phase gradient *decreases* rather than increases, as discussed below.

PHASING DOWN (s = 1 Phase Distributions)

By "phasing down" we mean the process of modifying the edge phase θ_M to achieve a new equilibrium phase gradient that is smaller than the initial gradient, $\Delta\theta_n < \Delta\phi_0$. Phasing down corresponds to the evolution of an $s = 1$ phase distribution (cf. Fig. 5).

From Eqs. (19), (21), and (23) (assuming again that $F > 0$),

$$\Delta\theta_n = \Delta\phi_0 - [2\pi - \alpha_M(0)]/M, \tag{B22a}$$

subject to the requirement that

$$(\pi - 2\Delta\phi_0) < \alpha_M(0) \leqslant 2\pi, \tag{B22b}$$

where $\Delta\phi_0$, $\Delta\theta_n$, and $\alpha_M(0)$ are defined as in Eq. (B17). The lower limit on $\Delta\theta_n$ established by Eq. (B22) is

$$\Delta\theta_n > [\Delta\phi_0 - (\pi + 2\Delta\phi_0)/M]. \tag{B23}$$

For example we assume $(\Delta\phi_0, M) = (60°, 9)$, as in Eq. (B19), and that the edge phasing is step-increased by

$$\alpha_M(0) = 1.01\ (\pi - 2\Delta\phi_0) = 60.6°. \tag{B24}$$

We find from Eqs. (B19), (B22a), and (B24) that the lattice eventually establishes a uniform phase gradient

$$\Delta\theta_n = 60° + (60.6° - 360°)/9 = 26.73°, \tag{B25}$$

just greater than the lower limit obtained from Eq. (B23), $\Delta\theta_n > 26.67°$.

We have seen that step-increasing the edge phase θ_M by 59.4° increases the phase gradient from 60° per module to 66.6° per module (cf. Eqs. (B19), (B20), and (B21)). A slightly larger edge phase increase of 60.6° decreases the phase gradient from 60° per module to 27° per module (Eqs. (B24) and (B25)).

PHASING LIMITS AND MULTISTEP PHASING PROCESSES

Starting from an initial phase gradient of $\Delta\phi_0$ per module, it follows from Eqs. (B18) and (B23) that there is no step-change in edge phase θ_M that will develop a phase gradient outside the range

$$[\Delta\phi_0 - (\pi + 2\Delta\phi_0)/M] < \Delta\theta_n < [\Delta\phi_0 + (\pi - 2\Delta\phi_0)/M]. \tag{B26}$$

Assuming for example that $(\Delta\phi_0, M) = (60°, 9)$ we obtain

$$26.67° < \Delta\theta_n < 66.67°. \tag{B27}$$

This apparent limitation on the range of $\Delta\theta_n$ is actually readily overcome. A multistep process can be used to sweep the phase gradient outside the range indicated by Eq. (B26).

Considering the phasing up process, for example, we generalize Eq. (B17) as follows:

$$\Delta\theta_n^{(i+1)} = \Delta\theta_n^{(i)} + [\alpha_M^{(i+1)}/M], \tag{B28a}$$

subject to the requirement that

$$0 \leqslant \alpha_M^{(i+1)} < [\pi - 2\Delta\theta_n^{(i)}], \tag{B28b}$$

where

$$\Delta\theta_n^{(0)} \equiv \Delta\phi_0, \tag{B28c}$$

and where $\Delta\theta_n^{(i)}$, $i = 1, 2, \ldots$, is the equilibrium phase gradient that evolves after the ith step-increase in edge phasing, $\alpha_M^{(i)}$.

Continuing our previous example, we find from Eqs. (B28), (B19), (B20), and (B21) that

$$\left.\begin{aligned}\alpha_M^{(1)} &= 59.4°\\ \Delta\theta_n^{(1)} &= 66.6°\end{aligned}\right\}. \tag{B29}$$

A new phase gradient $\Delta\theta_n^{(2)} > \Delta\theta_n^{(1)}$ may be established by initiating another step-increase in edge phasing, so long as we observe the constraint imposed by Eq. (B28b). Choosing, for example,

$$\alpha_M^{(2)} = 0.99[\pi - 2\Delta\theta_n^{(1)}] = 46.33°, \tag{B30}$$

we establish a new equilibrium phase gradient

$$\Delta\theta_n^{(2)} = 66.6° + (46.33°/9) = 71.75°, \tag{B31}$$

once the transient has decayed. The process may be continued, and ever-increasing phase gradients thereby achieved.

We obtain the multistep prescription for phasing down by generalizing Eq. (B22),

$$\Delta\theta_n^{(i+1)} = \Delta\theta_n^{(i)} - [2\pi - \alpha_M^{(i+1)}]/M, \tag{B32a}$$

subject to the requirement that

$$[\pi - 2\Delta\theta_n^{(i)}] < \alpha_M^{(i+1)} \leqslant 2\pi, \tag{B32b}$$

where $\Delta\theta_n^{(i)}$ and $\alpha_M^{(i+1)}$ are defined as in Eq. (B28).

The maximum increase in the phase gradient when phasing up is computed from Eq. (B28) as

$$[\Delta\theta_n^{(i+1)} - \Delta\theta_n^{(i)}] < [\pi - 2\Delta\theta_n^{(i)}]/M. \tag{B33}$$

The maximum decrease in the phase gradient when phasing down is obtained from Eq. (B32) as

$$[\Delta\theta_n^{(i)} - \Delta\theta_n^{(i+1)}] < [\pi + 2\Delta\theta_n^{(i)}]/M. \tag{B34}$$

Comparing Eqs. (B33) and (B34) we see that phasing down the lattice generally requires fewer steps than phasing up. Considering our previous example, Eq. (B19), we see that the lattice can be phased down $(60° - 26.7°) = 33.3°$ in a single step. By contrast, a single step-change in the edge phasing can phase up the gradient by no more than $(66.6° - 60°) = 6.6°$.

An important conclusion derivable directly from Eq. (B33) is that as $\Delta\theta_n^{(i)}$ approaches 90° per module, $[\Delta\theta_n^{(i+1)} - \Delta\theta_n^{(i)}]$ approaches zero, and no further increases in the phase gradient are achievable. Thus, phase gradients $90° \leqslant \Delta\theta_n < 180°$ are unattainable for positively coupled lattices.

Our discussion following from Eq. (B17) pertains only to positively coupled lattices, $F > 0$. A parallel formulation for $F < 0$ shows that

- phase gradients $0° \leqslant \Delta\theta_n < 90°$ are unattainable with negatively coupled lattices, and
- negatively coupled lattices can be phased up over the range $90° \leqslant \Delta\theta_n \leqslant 180°$ much more rapidly than they can be phased down.

Appendix C
TRANSIENT ANALYSIS

In this appendix we derive an exact solution to the equation

$$\theta_n(\tau + 1) = \frac{1}{2}[\theta_{n+1}(\tau) + \theta_{n-1}(\tau)], \tag{C1}$$

subject to the initial conditions

$$\theta_n(\tau) = n\Delta\phi_0, \; n = 1, 2, \ldots M, \; \tau < 0, \tag{C2}$$

and boundary conditions

$$\left.\begin{aligned} \theta_0(\tau) &= 0 \\ \theta_M(\tau) &= M\Delta\theta_n(\infty) \end{aligned}\right\} \; \tau \geqslant 0. \tag{C3}$$

Also, the equilibrium solution of Eq. (C1) in the limit of infinite time is given by

$$\theta_n(\infty) = n\Delta\theta_n(\infty), \tag{C4}$$

where $\Delta\theta_n(\infty)$ is a constant independent of n.

We begin our solution of Eq. (C1) by transforming to a new phase variable $\psi_n(\tau)$, subtracting the known equilibrium value $\theta_n(\infty)$ from $\theta_n(\tau)$,

$$\psi_n(\tau) \equiv \theta_n(\tau) - \theta_n(\infty) = \theta_n(\tau) - n\Delta\theta_n(\infty). \tag{C5}$$

Thus, $\psi_n(\tau)$ represents just the transient part of $\theta_n(\tau)$,

$$\lim_{\tau\to\infty} \psi_n(\tau) = 0. \tag{C6}$$

Applying Eq. (C5) to Eq. (C1) we obtain an identical difference equation for $\psi_n(\tau)$,

$$\psi_n(\tau + 1) = \frac{1}{2}[\psi_{n+1}(\tau) + \psi_{n-1}(\tau)]. \tag{C7}$$

The new boundary and initial conditions are obtained from Eqs. (C2), (C3), and (C5) as

$$\psi_0(\tau) = \psi_M(\tau) = 0, \tag{C8}$$

and

$$\psi_{no} \equiv \psi_n(0) = n[\Delta\phi_0 - \Delta\theta_n(\infty)], \; n = 1, 2, \ldots (M - 1). \tag{C9}$$

The point of our variable transformation, Eq. (C5), is to provide us with homogeneous boundary conditions, Eq. (C8), after which the initial value problem becomes solvable by separation of variables.

We look for solutions to Eq. (C7) of the form

$$\psi_n(\tau) = Z_n f(\tau). \tag{C10}$$

Substituting Eq. (C10) into Eq. (C7) we obtain

$$Z_n f(\tau + 1) = \frac{1}{2}(Z_{n+1} + Z_{n-1}) f(\tau).$$

Thus,

$$f(\tau + 1)/f(\tau) = (Z_{n+1} + Z_{n-1})/2Z_n = \lambda, \tag{C11}$$

where the parameter λ is dependent on neither τ nor n. From Eq. (C11)

$$f(\tau + 1) = \lambda f(\tau). \tag{C12}$$

Equation (C12) is solved either by inspection or by standard difference equation methods to obtain

$$f(\tau) = f(0)\lambda^{\tau}, \tag{C13}$$

where $f(0)$ is an undetermined constant.

Equation (C11) also provides us with an algebraic eigenvalue equation for Z_n,

$$\frac{1}{2}(Z_{n+1} + Z_{n-1}) = \lambda Z_n, \quad n = 1, 2, \ldots (M-1), \tag{C14}$$

where, from Eqs. (C8) and (C10),

$$Z_0 = Z_M = 0. \tag{C15}$$

As may be verified by substitution, the eigenvalues λ_k and corresponding eigenvectors $Z_n^{(k)}$ of Eq. (C14) are

$$\lambda_k = \cos(k\pi/M), \tag{C16}$$

and

$$Z_n^{(k)} = (2/M)^{1/2} \sin(\pi kn/M), \tag{C17}$$

for $k = 1, 2, \ldots (M-1)$. Eigenvectors (C17) satisfy the orthogonality condition

$$\sum_{n=1}^{M-1} Z_n^{(k)} Z_n^{(l)} = \delta_{k,l} = \begin{cases} 1, & k = l \\ 0, & k \neq l. \end{cases} \tag{C18}$$

The general solution of Eq. (C7) is obtained from Eqs. (C10) and (C13) as

$$\psi_n(\tau) = \sum_{k=1}^{M-1} A_k Z_n^{(k)} \lambda_k^{\tau}, \tag{C19}$$

where the constants A_k must be determined from the initial conditions. We set $\tau = 0$ in Eq. (C19), multiply by $Z_n^{(l)}$, and sum over index n to obtain

$$\sum_{n=1}^{M-1} \psi_n(0) Z_n^{(l)} = \sum_{k=1}^{M-1} A_k \left[\sum_{n=1}^{M-1} Z_n^{(k)} Z_n^{(l)} \right]. \tag{C20}$$

Thus, from Eqs. (C18) and (C20),

$$A_k = \sum_{n=1}^{M-1} \psi_{n0} Z_n^{(k)}. \tag{C21}$$

Substituting Eq. (C9) for ψ_{n0} and Eq. (C17) for $Z_n^{(k)}$ into Eq. (C21) we obtain

$$A_k = (2/M)^{1/2}[\Delta\theta_n(\infty) - \Delta\phi_0] \sum_{n=1}^{M-1} n \sin(\pi kn/M). \tag{C22}$$

The summation in Eq. (C22) can be performed analytically, with the result

$$A_k = (M/2)^{1/2}[\Delta\theta_n(\infty) - \Delta\phi_0](-1)^k \cot(\pi k/2M). \tag{C23}$$

From Eqs. (C19), (C23), (C16), and (C17),

$$\psi_n(\tau) = \sum_{k=1}^{M-1} \psi_n^{(k)}(\tau), \tag{C24}$$

where

$$\psi_n^{(k)}(\tau) = [\Delta\theta_n(\infty) - \Delta\phi_0](-1)^k \cot\left(\frac{\pi k}{2M}\right) \sin\left(\frac{\pi kn}{M}\right) \left[\cos\left(\frac{k\pi}{M}\right)\right]^{\tau}. \tag{C25}$$

Since

$$\cos\left[\frac{k\pi}{M}\right] = -\cos\left[\frac{(M-k)\pi}{M}\right]$$

we see from Eq. (C25) that $\psi_n^{(k)}(\tau)$ has the same time dependence as $\psi_n^{(M-k)}(\tau)$. This suggests writing Eq. (C24) in the form

$$\psi_n(\tau) = \sum_{k=1}^{[M/2]} [\psi_n^{(k)}(\tau) + \psi_n^{(M-k)}(\tau)], \tag{C26}$$

where $[M/2]$ is the integer part of $M/2$,

$$[M/2] = \begin{cases} (M/2) \ , & M \text{ even} \\ (M-1)/2 \ , & M \text{ odd.} \end{cases} \tag{C27}$$

We can show from Eqs. (C25) and (C26) that

$$\psi_n(\tau) = 2[\Delta\theta_n(\infty) - \Delta\phi_0] \sum_{k=1}^{[M/2]} (-1)^k \left[\frac{\sin(nk\pi/M)}{\sin(k\pi/M)}\right] [\cos(k\pi/M)]^{\tau+\mu}, \tag{C28}$$

where

$$\mu \equiv \frac{1}{2}[1 + (-1)^{n+\tau+M}]. \tag{C29}$$

Equation (C28) is the exact solution of Eq. (C1), subject to Eqs. (C2) and (C3), the initial conditions and boundary conditions, respectively.

Appendix D
UNEQUAL FORWARD AND BACKWARD COUPLING

FORMULATION

The equilibrium phase distribution of the CAM network is the solution of Eq. (13),

$$\Delta\theta_{n+1} = \Delta\theta_n + \epsilon_n \tan \frac{1}{2} (\Delta\theta_{n+1} + \Delta\theta_n), \tag{D1}$$

where

$$\epsilon_n \equiv 2 \left(\frac{F_n - B_n}{F_n + B_n} \right) \ll 1. \tag{D2}$$

We now define a quantity $\Delta\phi_n$ that measures the degree to which the actual phase gradient $\Delta\theta_n$ departs from the ideal, i.e.,

$$\Delta\phi_n = \Delta\theta_n - \Delta\theta_n^0. \tag{D3}$$

From Eqs. (D1) and (D3)

$$\Delta\phi_{n+1} = \Delta\phi_n + \epsilon_n \tan \left[\Delta\theta_n^0 + \frac{1}{2} (\Delta\phi_{n+1} + \Delta\phi_n) \right], \tag{D4}$$

where, from Eq. (19),

$$\Delta\theta_n^0 = \Delta\phi - s(2\pi/M), \; n = 1, 2, \ldots M. \tag{D5}$$

If the CAM network is to be useful for exciting a phased array antenna, it must be true that

$$\frac{1}{2} (\Delta\phi_{n+1} + \Delta\phi_n) \ll \Delta\theta_n^0, \tag{D6}$$

from which we can show that

$$\tan \left[\Delta\theta_n^0 + \frac{1}{2} (\Delta\phi_{n+1} + \Delta\phi_n) \right] \simeq \tan \Delta\theta_n^0 + \frac{1}{2} (\Delta\phi_{n+1} + \Delta\phi_n) \sec^2 \Delta\theta_n^0. \tag{D7}$$

From Eqs. (D4) and (D7),

$$\Delta\phi_{n+1} = \Delta\phi_n + \epsilon_n \tan \Delta\theta_n^0 + \frac{1}{2} \epsilon_n (\Delta\phi_{n+1} + \Delta\phi_n) \sec^2 \Delta\theta_n^0. \tag{D8}$$

Since development of an exact closed form solution to Eq. (D8) appears quite difficult, we propose an iterative solution,

$$\Delta\phi_{n+1}^{(i+1)} = \Delta\phi_n^{(i+1)} + \epsilon_n \tan \Delta\theta_n^0 + \frac{1}{2} \epsilon_n (\Delta\phi_{n+1}^{(i)} + \Delta\phi_n^{(i)}) \sec^2 \Delta\theta_n^0. \tag{D9}$$

In the limit of fabricationally perfect modules,

$$\lim_{\epsilon_n \to 0} \Delta\theta_n = \Delta\theta_n^0. \tag{D10}$$

The zero-order iterate $\Delta\phi_n^{(0)}$ is thus obtained from Eqs. (D3) and (D10)

$$\Delta\phi_n^{(0)} = 0. \tag{D11}$$

The first-order iterate follows from Eqs. (D9) and (D11),

$$\Delta\phi_{n+1}^{(1)} = \Delta\phi_n^{(1)} + \epsilon_n \tan \Delta\theta_n^0. \tag{D12}$$

We simplify notation by dropping the superscript on $\Delta\phi_n^{(1)}$ and by setting $s = 0$ in Eq. (D5) to obtain

$$\Delta\phi_{n+1} = \Delta\phi_n + \epsilon_n \tan \Delta\phi. \tag{D13}$$

The solution of Eq. (D13) is

$$\Delta\phi_n = K - \tan \Delta\phi \sum_{p=n}^{M} \epsilon_p, \quad n = 1, 2, \ldots M, \tag{D14}$$

as may be verified by back substitution into Eq. (D13). The constant K in Eq. (D14) is independent of the module index n.

Since the values of θ_0 and θ_M are imposed by the phase control element (cf. Fig. 2), they are independent of whether the modules are fabricationally perfect or imperfect; thus,

$$\begin{aligned} \theta_0 &= \theta_0^0 \\ \theta_M &= \theta_M^0. \end{aligned} \tag{D15}$$

Defining

$$\phi_n \equiv \theta_n - \theta_n^0, \tag{D16}$$

boundary conditions on ϕ_n are obtained from Eqs. (D15) and (D16),

$$\phi_0 = \phi_M = 0. \tag{D17}$$

We impose these boundary conditions on Eq. (D14) to determine the value of K.

Toward determining the proper value of K we note that

$$\sum_{n=1}^{M} \Delta\phi_n = \sum_{n=1}^{M} (\phi_n - \phi_{n-1}) = (\phi_M - \phi_0) = 0, \tag{D18}$$

where the final equality in Eq. (D18) follows from Eq. (D17). However, from Eq. (D14),

$$\sum_{n=1}^{M} \Delta\phi_n = MK - \tan \Delta\phi \sum_{n=1}^{M} \sum_{p=n}^{M} \epsilon_p. \tag{D19}$$

Thus, from Eqs. (D18) and (D19)

$$K = \frac{1}{M} \sum_{r=1}^{M} \sum_{p=r}^{M} \epsilon_p \tan \Delta\phi. \tag{D20}$$

Substituting Eq. (D20) into Eq. (D14) we obtain the general first-order approximate solution of Eq. (D8),

$$\Delta\phi_n = \left[\frac{1}{M} \sum_{r=1}^{M} \sum_{p=r}^{M} \epsilon_p - \sum_{p=n}^{M} \epsilon_p \right] \tan \Delta\phi, \quad n = 1, 2, \ldots M. \tag{D21}$$

We obtain the solution for ϕ_n by noting that, analogous to Eq. (D18),

$$\sum_{r=1}^{n} \Delta\phi_r = (\phi_n - \phi_0) = \phi_n, \quad n = 1, 2, \ldots M. \tag{D22}$$

From Eqs. (D21) and (D22)

$$\phi_n = \left[\frac{n}{M}\sum_{r=1}^{M}\sum_{p=r}^{M}\epsilon_p - \sum_{r=1}^{n}\sum_{p=r}^{M}\epsilon_p\right]\tan\Delta\phi,\quad n = 1, 2, \ldots M. \tag{D23}$$

Equation (D23) correctly reproduces the boundary condition at $n = M$, namely $\phi_M = 0$. However, we should not be worried that the boundary condition at $n = 0$ is not reproduced since Eq. (D22) (from which Eq. (D23) was derived) is not valid for $n = 0$.

Finally, we should not be concerned that the quantity ϵ_M appearing in some of the above equations is not strictly defined, since terms in ϵ_M identically cancel from our final results, Eqs. (D21) and (D23). Thus, Eqs. (D21) and (D22) can each be written in a form in which ϵ_M does not appear:

$$\Delta\phi_n = \begin{cases}\left\{\frac{1}{M}\sum_{r=1}^{M-1}\sum_{p=r}^{M-1}\epsilon_p - \sum_{p=n}^{M-1}\epsilon_p\right\}\tan\Delta\phi & , n = 1, 2, \ldots (M-1)\\ \left\{\frac{1}{M}\sum_{r=1}^{M-1}\sum_{p=r}^{M-1}\epsilon_p\right\}\tan\Delta\phi & , n = M\end{cases}$$

$$\phi_n = \begin{cases}\left\{\left(\frac{n}{m}\right)\sum_{r=1}^{M-1}\sum_{p=r}^{M-1}\epsilon_p - \sum_{r=1}^{n}\sum_{p=r}^{M-1}\epsilon_p\right\}\tan\Delta\phi & , n = 1, 2, \ldots (M-1)\\ 0 & , n = M.\end{cases}$$

The latter two equations evaluate identically to Eqs. (D21) and (D23), respectively. We generally prefer to work with Eqs. (D21) and (D23) for obvious reasons.

CONSTANT COUPLING RATIO

We presently assume that

$$\epsilon_n = \epsilon,\quad n = 1, 2, \ldots (M-1), \tag{D24}$$

i.e., we assume that all modules in the CAM network are identical, even though they are imperfect. (We recall that, by definition, a perfect module is one for which $F_n = B_n$, i.e., $\epsilon_n = 0$, $n = 1, 2, \ldots (M-1)$.)

It follows from Eq. (D24) that the summations appearing in Eq. (D21) are readily evaluated,

$$\frac{1}{M}\sum_{r=1}^{M}\sum_{p=r}^{M}\epsilon_p = \epsilon\left\lfloor\frac{M+1}{2}\right\rfloor$$

$$\sum_{p=n}^{M}\epsilon_p = (M - n + 1)\epsilon. \tag{D25}$$

Substituting Eq. (D25) into Eq. (D21),

$$\Delta\phi_n \simeq \Delta\phi_n^{(1)} = \epsilon a_n,\quad n = 1, 2, \ldots M, \tag{D26}$$

where

$$a_n \equiv [n - (M+1)/2]\tan\Delta\phi. \tag{D27}$$

We see from Eq. (D26) that the error in the intermodule phasing is minimum at the array center and maximum at its edges.

In Fig. 11 we compare values predicted by Eq. (D26) with a computer solution of Eq. (4), for the parameter values

$$(\epsilon, \Delta\phi, M) = (10^{-2}, 65^0, 9). \tag{D28}$$

We recall that Eq. (D26) is a first-order approximation. Later in this appendix we calculate a second-order approximation that greatly reduces the discrepancy between the numerical and analytical calculations evidenced in Fig. 11.

TAPERED COUPLING RATIO

Perhaps the simplest type of nonuniform network is the linear taper, for which

$$\epsilon_n = n\epsilon_1, \quad n = 1, 2, \ldots (M-1). \tag{D29}$$

From Eqs. (D29) and (D13),

$$\Delta\phi_{n+1} = \Delta\phi_n + n\epsilon_1 \tan \Delta\phi. \tag{D30}$$

It can be shown that the summations appearing in Eq. (D21) evaluate as follows,

$$\sum_{p=n}^{M} \epsilon_p = \left[\frac{\epsilon_1}{2}\right] [M(M+1) - n(n-1)], \tag{D31}$$

and

$$\frac{1}{M} \sum_{r=1}^{M} \sum_{p=r}^{M} \epsilon_p = (\epsilon_1/6)\ (M+1)\ (2M+1). \tag{D32}$$

From Eqs. (D21), (D31), and (D32),

$$\Delta\phi_n = \epsilon_1 b_n, \quad n = 1, 2, \ldots M, \tag{D33}$$

where

$$b_n \cong \left[\frac{1}{6}\right] [3n(n-1) - (M^2-1)] \tan \Delta\phi. \tag{D34}$$

To obtain $\Delta\phi_n$ in degrees Eq. (D33) (like Eq. (D26)) must be multiplied by $(180/\pi)$.

We note that the value of n for which Eq. (D33) is equal to zero may be approximated as

$$n_0 \simeq 0.5 + 0.577\ M, \quad \Delta\phi_{n_0} = 0. \tag{D35}$$

In Fig. D1 we compare values predicted by Eq. (D33) with a computer solution of Eq. (4), for the parameter values

$$(\epsilon_1, \Delta\phi, M) = (0.0025, 65°, 9).$$

The predictions of the approximate analytic solution, Eq. (D33), appear quite close to the exact numerical solution.

CONSTANT COUPLING RATIO: SECOND-ORDER APPROXIMATION

From Eqs. (D9) and (D24) we obtain

$$\Delta\phi_{n+1}^{(2)} = \Delta\phi_n^{(2)} + \epsilon \tan \Delta\theta_n^0 + \frac{1}{2}\epsilon(\Delta\phi_{n+1}^{(1)} + \Delta\phi_n^{(1)}) \sec^2 \Delta\theta_n^0, \tag{D36}$$

where $\Delta\phi_{n+1}^{(1)}$ is the first-order approximation given by Eq. (D26). From Eqs. (D26) and (D27)

$$\frac{1}{2}(\Delta\phi_{n+1}^{(1)} + \Delta\phi_n^{(1)}) = \epsilon\left[n - \frac{M}{2}\right] \tan \Delta\phi. \tag{D37}$$

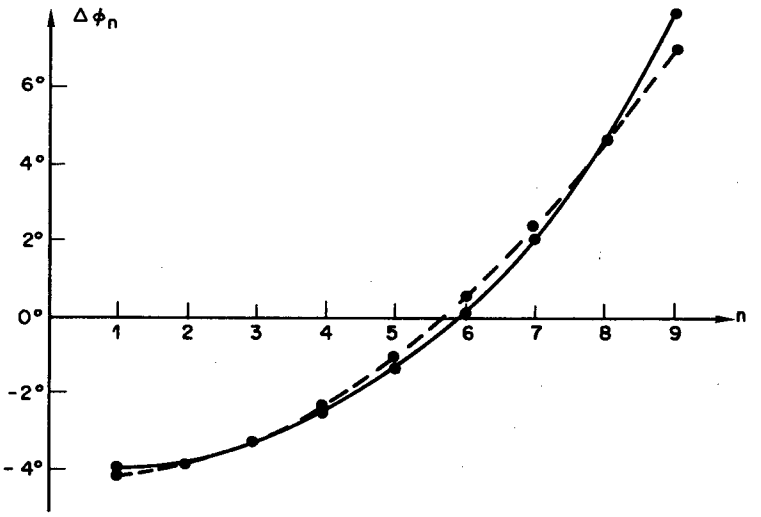

Fig. D1 — Equilibrium phase error for an 8-module feed with a linearly tapered imperfection. Parameter values assumed are $(\epsilon_1, \Delta\phi, M) = (0.0025, 65°, 9)$. Solid curve obtained by numerical solution of Eq. (4); dashed curve obtained by first-order approximation, Eq. (D33). Quantity $\Delta\phi_n$ is defined only at integral values of n.

Substituting Eq. (D37) into Eq. (D36),

$$\Delta\phi_{n+1} = \Delta\phi_n + \epsilon \tan \Delta\phi + \epsilon^2\left(n - \frac{M}{2}\right) \sec^2 \Delta\phi \tan \Delta\phi, \tag{D38}$$

where we simplify notation by dropping the superscript from $\Delta\phi_n^{(2)}$ and by substituting $\Delta\phi$ for $\Delta\theta_n^0$ (i.e., setting $s = 0$ in Eq. (D5)). Equation (D38) may be written as

$$\Delta\phi_{n+1} = \Delta\phi_n + E \tan \Delta\phi + nE_1 \tan \Delta\phi, \tag{D39}$$

where, by definition,

$$E \equiv \epsilon\left(1 - \frac{1}{2}\epsilon M \sec^2 \Delta\phi\right)$$

$$E_1 \equiv \epsilon^2 \sec^2 \Delta\phi. \tag{D40}$$

The solution of Eq. (D39) may be written by superposing the solutions of Eqs. (D13) and (D30). Thus, from Eqs. (D26) and (D33),

$$\Delta\phi_n \simeq \Delta\phi_n^{(2)} = Ea_n + E_1 b_n, \tag{D41}$$

where a_n and b_n are given by Eqs. (D27) and (D34), respectively. We can show from Eqs. (D41) and (D26) that

$$[\Delta\phi_n^{(2)} - \Delta\phi_n^{(1)}] = \frac{1}{2}\{[n - (M+1)/2]^2 - (M^2 - 1)/12\}\epsilon^2 \sec^2 \Delta\phi \tan \Delta\phi. \tag{D42}$$

As shown in Fig. 11, the second-order approximation brings our analytical results much closer to the exact numerical solution of Eq. (4).

RANDOM COUPLING

Rather than take ϵ_n as a known function of n (e.g., Eqs. (D24) and (D29)), we now assume that the coupling coefficients F_n and B_n are independent, identically distributed, random variables. The quantity ϵ_n is thus also a random variable as a consequence of Eq. (D2).

We denote the mean value and variance of a random variable X as μ_x and σ_x^2, respectively. Thus, by assumption, $\mu_F = \mu_B$ and $\sigma_F = \sigma_B$, while μ_ϵ and σ_ϵ are independent of the module index n,

$$\mu_\epsilon = E\{\epsilon_n\}, \quad n = 1, 2, \ldots (M-1)$$
$$\sigma_\epsilon^2 = E\{(\epsilon_n - \mu_\epsilon)^2\}, \quad n = 1, 2, \ldots (M-1). \tag{D43}$$

The statistical expectation operator is denoted as $E[\cdot]$ in Eq. (D43).

Since a simple relationship exists between ϵ_n, F_n, and B_n, Eq. (D2), we might expect simple relationships to exist between their mean values and variances. These relationships are derived as Eqs. (E11) to (E15).

To simplify our notation we define

$$\mu_n \equiv E\{\Delta\phi_n\},$$
$$P_n^2 \equiv E\{\Delta\phi_n^2\}, \tag{D44}$$
$$\sigma_n^2 \equiv \{(\Delta\phi_n - \mu_n)^2\} = (P_n^2 - \mu_n^2).$$

An expression for μ_n, the mean phase error, is obtained by applying the expectation operator to Eq. (D21). Since the expectation operator commutes with the summation operations we find

$$\mu_n = \left\{\frac{1}{M}\sum_{r=1}^{M}\sum_{p=r}^{M}\mu_\epsilon - \sum_{p=n}^{M}\mu_\epsilon\right\}\tan\Delta\phi. \tag{D45}$$

Since the random variables ϵ_n are identically distributed, their mean values μ_ϵ are all identical (Eq. (D43)). Thus, Eq. (D45) evaluates precisely as for the constant coupling ratio problem, Eq. (D24). As a simple adaptation of Eq. (D26) we find that

$$\mu_n = \mu_\epsilon[n - (M+1)/2]\tan\Delta\phi, \quad n = 1, 2, \ldots (M-1). \tag{D46}$$

From Eqs. (D46) and (E14)

$$\mu_n = 10^{-4}A^2[n - (M+1)/2]\tan\Delta\phi, \tag{D47}$$

where A is the percentage fabricational accuracy, as defined by Eq. (E13).

For example, assuming that

$$(A, M, \Delta\phi) = (1\%, 9, 45°), \tag{D48}$$

we find the maximum expected phase error is just

$$\max_n \mu_n = \mu_M = 4 \times 10^{-4}\ (\text{rad}) = 0.023°. \tag{D49}$$

Thus the mean phase increment is very nearly a constant,

$$E\{\Delta\theta_n\} = \mu_n + \Delta\phi \simeq \Delta\phi. \tag{D50}$$

From Eq. (D50)

$$E\{\theta_n\} \simeq n\Delta\phi. \tag{D51}$$

It is of interest to determine the extent to which we may expect the phase distribution $\Delta\theta_n$ to deviate from its mean, Eq. (D50). For this purpose we need to evaluate the second-order statistic $E[\Delta\theta_n^2] - E[\Delta\theta_n]^2$. First, we note that

$$E\{\Delta\theta_n^2\} = E\{\Delta\phi_n^2\} = P_n^2, \tag{D52}$$

as a consequence of the fact that

$$\Delta\theta_n = \Delta\phi_n + \Delta\phi. \tag{D53}$$

We recall that $\Delta\phi$ in Eq. (D53) is deterministic and is determined by the boundary condition, Eq. (5); i.e., $\Delta\phi$ is determined by the phase control element in Fig. 2.

From Eq. (D21),

$$P_n^2 = \tan^2 \Delta\phi \cdot p_n, \tag{D54}$$

where

$$p_n = E\left\{\left[\frac{1}{M}\sum_{r=1}^{M}\sum_{p=r}^{M}\epsilon_p - \sum_{p=n}^{M}\epsilon_p\right]\left[\frac{1}{M}\sum_{s=1}^{M}\sum_{k=s}^{M}\epsilon_k - \sum_{k=n}^{M}\epsilon_k\right]\right\}. \tag{D55}$$

Four terms are obtained when the multiplication inside the expectation operator in Eq. (D55) is performed. Commuting the expectation operator with the summations, we find from Eq. (D55) that

$$p_n = L + R_n - M_n - E_n, \tag{D56}$$

where

$$L \equiv \frac{1}{M^2}\sum_{r=1}^{M}\sum_{s=1}^{M}\sum_{p=r}^{M}\sum_{k=s}^{M} E\{\epsilon_p\epsilon_k\}, \tag{D57}$$

$$R_n \equiv \sum_{p=n}^{M}\sum_{k=n}^{M} E[\epsilon_p\epsilon_k], \tag{D58}$$

$$M_n \equiv \frac{1}{M}\sum_{s=1}^{M}\left\{\sum_{p=n}^{M}\sum_{k=s}^{M} E[\epsilon_p\epsilon_k]\right\}, \tag{D59}$$

and

$$E_n \equiv \frac{1}{M}\sum_{r=1}^{M}\left\{\sum_{p=r}^{M}\sum_{k=n}^{M} E[\epsilon_p\epsilon_k]\right\}. \tag{D60}$$

Following our assumption that (F_n, B_n) are statistically independent of (F_m, B_m), for $n \neq m$, we find that

$$E[\epsilon_p\epsilon_k] = \sigma_\epsilon^2\delta_{p,k} = \begin{cases}\sigma_\epsilon^2, & p = k\\ 0, & p \neq k.\end{cases} \tag{D61}$$

With the definition

$$S_{uv} \equiv \sigma_\epsilon^2 \sum_{p=u}^{M}\sum_{k=v}^{M}\delta_{p,k}, \tag{D62}$$

it follows that Eqs. (D57) to (D60) may be written as

$$L = \frac{1}{M^2}\sum_{r=1}^{M}\sum_{s=1}^{M} S_{rs}, \tag{D63}$$

$$R_n = S_{nn}, \tag{D64}$$

$$M_n = \frac{1}{M}\sum_{s=1}^{M} S_{ns}, \tag{D65}$$

and

$$E_n = \frac{1}{M}\sum_{r=1}^{M} S_{rn}. \tag{D66}$$

It follows from Eq. (D62) that $S_{uv} = S_{vu}$. Thus, from Eqs. (D65) and (D66), we see that $M_n = E_n$.

It can be shown from Eq. (D62) that

$$S_{uv} = \sigma_\epsilon^2[(M+1) - \max(u, v)], \tag{D67}$$

where $\max(u, v)$ denotes the larger of u and v,

$$\max(u, v) = \begin{cases} u, & u > v \\ v, & v > u. \end{cases} \tag{D68}$$

It can be shown from Eqs. (D63) to (D67) that

$$L = \sigma_\epsilon^2 \cdot \frac{1}{6} M^{-1}(M+1)(2M+1), \tag{D69}$$

$$R_n = \sigma_\epsilon^2(M+1-n), \tag{D70}$$

and

$$M_n = E_n = \sigma_\epsilon^2 \cdot \frac{1}{2} M^{-1}[M(M+1) - n(n-1)]. \tag{D71}$$

Collecting terms, it follows from Eqs. (D54), (D56), (D69), (D70), and (D71), that

$$P_n^2 = E[(\Delta\phi_n)^2] = (\sigma_\epsilon^2 \tan^2 \Delta\phi)(1 + M^{-1})\left[\frac{1}{3}\left(M + \frac{1}{2}\right) - n + n^2(M+1)^{-1}\right]. \tag{D72}$$

We complete the square on n in Eq. (D72), to obtain

$$P_n = \sigma_\epsilon \tan \Delta\phi \left\{\frac{1}{12} M(1 - M^{-2}) + M^{-1}[n - (M+1)/2]^2\right\}^{1/2}. \tag{D73}$$

Equation (D73) clearly displays the expected symmetry about $n = (M+1)/2$.

From Eqs. (D73) and (E15), and multiplying by $(180/\pi)$, we obtain

$$P_n = \frac{1}{1.234} A \tan \Delta\phi \left\{\frac{1}{12} M(1 - M^{-2}) + M^{-1}[n - (M+1)/2]^2\right\}^{1/2}, \text{ degrees.} \tag{D74}$$

Multiplying Eq. (D47) by $(180/\pi)$,

$$\mu_n = \frac{1}{175} A^2 \tan \Delta\phi [n - (M+1)/2], \text{ degrees.} \tag{D75}$$

Froms Eqs. (D44), (D74), and (D75)

$$\sigma_n^2 = (P_n^2 - \mu_n^2) \simeq P_n^2, \tag{D76}$$

so long as

$$M A^2 \ll 2 \times 10^4. \tag{D77}$$

Assuming that Eq. (D77) is valid, and also that

$$M^{-2} \ll 1, \tag{D78}$$

we find from Eqs. (D74), (D76), (D77), and (D78) that

$$\sigma_n \equiv \{E[(\Delta\phi_n)^2] - [E(\Delta\phi_n)]^2\}^{1/2} \tag{D79}$$

$$\sigma_n = 0.234 A \tan \Delta\phi M^{1/2}\{1 + 12M^{-2}[n - (M+1)/2]^2\}^{1/2}, \text{ degrees,} \quad n = 1, 2, \ldots M. \tag{D80}$$

We recall that A in Eq. (D80) is the percentage fabricational accuracy, defined by Eq. (E13); $(M-1)$ is the number of modules; $M\Delta\phi$ is the phase shift established by the phase control element in Fig. 2; n is the module index; σ_n is the root-mean-square (RMS) deviation of $\Delta\theta_n = \theta_n - \theta_{n-1}$ from its desired value, $\Delta\theta_n = \Delta\phi$.

It follows from Eq. (D80) that the RMS phase error is minimum at the center of the array and maximum at its edges. From Eq. (D80)

$$\min_n \sigma_n = 0.234\ A\ \tan \Delta\phi \cdot M^{1/2},\ \text{degrees}, \tag{D81}$$

while

$$\max_n \sigma_n \simeq 2(1 - 0.75M^{-1})(\min_n \sigma_n),\ \text{degrees}. \tag{D82}$$

For the example of Eq. (D48) we find for the minimum and maximum RMS phase errors,

$$\min_n \sigma_n = \sigma_5 = 0.70° \tag{D83}$$

and

$$\max_n \sigma_n = \sigma_1 = \sigma_9 = 1.29°. \tag{D84}$$

Appendix E
RELATIONSHIPS BETWEEN COUPLING STATISTICS AND POWER SPLITTER ACCURACY

Our objective in this appendix is to derive expressions for the mean and variance of ϵ_n,

$$\epsilon_n = 2\left(\frac{F_n - B_n}{F_n + B_n}\right) \simeq \frac{F_n}{B_n} - 1, \tag{E1}$$

in terms of the mean and variance of the power split coefficients F_n and B_n.

As a matter of notation, the expectation operator is denoted as $E[\cdot]$. The mean and variance of random variable X are denoted as μ_x and σ_x^2, respectively. We assume that random variables F_n and B_n are independent and identically distributed. Thus

$$\begin{aligned} \mu_F &= \mu_B \\ \sigma_F &= \sigma_B, \end{aligned} \tag{E2}$$

for all values of n.

Our results are obtained as a special case of a theorem appearing on p. 141 of Ref. E1. We state the general form of the theorem first.

If the random variable Z is a function of the two random variables F and B,

$$Z = H(F, B), \tag{E3}$$

the mean and variance of Z may be approximated by the following:

$$\mu_z \simeq H(\mu_F, \mu_B) + \frac{1}{2}\left[(\partial_{FF}^2 H)\,\sigma_F^2 + (\partial_{BB}^2 H)\,\sigma_B^2\right] \tag{E4}$$

$$\sigma_z^2 \simeq (\partial_F H)^2\,\sigma_F^2 + (\partial_B H)^2\,\sigma_B^2. \tag{E5}$$

The partial derivatives $\partial_F = \dfrac{\partial}{\partial F}$, etc., in Eqs. (E4) and (E5) are evaluated at $(F, B) = (\mu_F, \mu_B)$.

For the special case

$$Z = F \cdot B^{-1}, \tag{E6}$$

and making use of Eq. (E2), we find from Eqs. (E4) and (E5) that

$$\mu_z \simeq 1 + (\sigma_F/\mu_F)^2, \tag{E7}$$

and

$$\sigma_z^2 \simeq 2(\sigma_F/\mu_F)^2. \tag{E8}$$

However, from Eqs. (E1) and (E6)

$$\mu_\epsilon = \mu_z - 1, \tag{E9}$$

and

$$\sigma_\epsilon^2 = \sigma_z^2. \tag{E10}$$

From Eqs. (E7) through (E10),

$$\mu_\epsilon \simeq (\sigma_F/\mu_F)^2, \tag{E11}$$

and

$$\sigma_\epsilon \simeq \sqrt{2}\ (\sigma_F/\mu_F). \tag{E12}$$

If we define the fabricational accuracy A as

$$A = 100\ (\sigma_F/\mu_F)\ \text{(percent)}, \tag{E13}$$

Eqs. (E11) and (E12) become

$$\mu_\epsilon = 10^{-4}\ A^2, \tag{E14}$$

and

$$\sigma_\epsilon = \sqrt{2} \times 10^{-2} A. \tag{E15}$$

For fabricational accuracies $A \simeq 1\%$, we see from Eqs. (E14) and (E15) that σ_ϵ is about two orders of magnitude larger than μ_ϵ. Thus, we are often able to ignore μ_ϵ, regarding ϵ as a zero-mean random variable.

$$E[\epsilon_p \epsilon_k] = \sigma_\epsilon^2 \delta_{p,k} = \begin{cases} \sigma_\epsilon^2\ , & p = k \\ 0\ , & p \neq k. \end{cases} \tag{D61}$$

REFERENCE

E1. P.L. Meyer, *Introductory Probability and Statistical Applications,* Second Edition (Addison-Wesley, Reading, Mass., 1970).

Appendix F
MODULES WITH SELF-COUPLING

We can show that the transient phase distribution of modules with self-coupling, Fig. 12, evolves according to the equation

$$e^{j\theta_n(\tau+1)} = N_n(\tau)[e^{j\theta_n(\tau)} + Be^{j\theta_{n+1}(\tau)} + Fe^{j\theta_{n-1}(\tau)}], \tag{F1}$$

analogous to Eq. (4). We simplify the analysis in the remainder of this appendix by assuming equal forward- and backward-coupling,

$$F = B. \tag{F2}$$

With the definitions

$$\Delta\theta_n(\tau) = \theta_n(\tau) - \theta_{n-1}(\tau), \tag{F3}$$

$$N \equiv N_n(\tau), \tag{F4}$$

$$\alpha \equiv \theta_n(\tau + 1) - \theta_n(\tau), \tag{F5}$$

$$A \equiv \frac{1}{2}[\Delta\theta_{n+1}(\tau) + \Delta\theta_n(\tau)], \tag{F6}$$

$$S \equiv \frac{1}{2}[\Delta\theta_{n+1}(\tau) - \Delta\theta_n(\tau)], \tag{F7}$$

Eq. (F1) may be written as

$$e^{j\alpha} = N(1 + 2Fe^{jS}\cos A). \tag{F8}$$

Taking the real and imaginary parts of Eq. (F8) we obtain

$$\sin\alpha = 2NF\cos A\ \sin S, \tag{F9}$$

and

$$\cos\alpha = N(1 + 2F\cos A\ \cos S). \tag{F10}$$

Dividing Eq. (F9) by Eq. (F10),

$$\tan\alpha = \left(\frac{2F\cos A}{1 + 2F\cos A\ \cos S}\right)\sin S. \tag{F11}$$

Inspection of numerous numerical solutions of Eq. (F1) shows that the spatial/temporal development of the phase distribution proceeds gradually after an initial short period of rapid changes. Thus,

$$|\alpha| = |\theta_n(\tau + 1) - \theta_n(\tau)| << 1, \quad \tau >> 1, \tag{F12}$$

and

$$|S| = \frac{1}{2}|\Delta\theta_{n+1}(\tau) - \Delta\theta_n(\tau)| << 1, \quad \tau >> 1. \tag{F13}$$

From Eqs. (F12) and (F5),

$$\tan\alpha \simeq \alpha = \theta_n(\tau + 1) - \theta_n(\tau). \tag{F14}$$

From Eqs. (F13) and (F7),

$$\sin S \simeq S = \frac{1}{2}[\Delta\theta_{n+1}(\tau) - \Delta\theta_n(\tau)], \tag{F15}$$

and

$$\cos S \simeq 1. \tag{F16}$$

From Eqs. (F13) and (F6),

$$A = \frac{1}{2}[\Delta\theta_{n+1}(\tau) + \Delta\theta_n(\tau)] \simeq \Delta\theta_n(\tau). \tag{F17}$$

Substituting Eqs. (F14) through (F17) into Eq. (F11) we obtain

$$[\theta_n(\tau + 1) - \theta_n(\tau)] \simeq \left(\frac{F \cos \Delta\theta_n}{1 + 2F \cos \Delta\theta_n}\right)[\Delta\theta_{n+1}(\tau) - \Delta\theta_n(\tau)]. \tag{F18}$$

Using our definition for $\Delta\theta_n(\tau)$, Eq. (F3), Eq. (F18) may be written as

$$[\theta_n(\tau + 1) - \theta_n(\tau)] = \frac{1}{2}C_n(\tau)[\theta_{n+1}(\tau) - 2\theta_n(\tau) + \theta_{n-1}(\tau)], \tag{F19}$$

where

$$C_n(\tau) = \left[1 + \frac{1}{2} F^{-1} \sec \Delta\theta_n(\tau)\right]^{-1}. \tag{F20}$$

Equation (F19) has the form of a 1-D heat flow equation in which the time and space derivatives have been replaced by finite differences. However, the solution of Eq. (F19) is complicated by the fact that the "diffusivity" $C_n(\tau)$ is a function both of space and of time. Further simplification is achieved by remembering that when $\tau >> 1$ the quantities $\Delta\theta_n(\tau)$ approach their equilibrium values,

$$\lim_{\tau\to\infty} \Delta\theta_n(\tau) = \Delta\phi, \tag{F21}$$

where we simplify notation by setting $s = 0$ in Eq. (19). From Eqs. (F19), (F20), and (F21)

$$\theta_n(\tau + 1) = \frac{1}{2}C[\theta_{n+1}(\tau) + \theta_{n-1}(\tau)] + (1 - C)\theta_n(\tau), \tag{F22}$$

where

$$C = \left[1 + \frac{1}{2} F^{-1} \sec \Delta\phi\right]^{-1}. \tag{F23}$$

In the limit $F \to \infty$ we see that $C \to 1$, and Eq. (F22) reduces as expected to Eq. (A10). More generally, we solve Eq. (F22) by the same separation-of-variables method we previously used to solve Eq. (A10), with the result

$$\psi_n(\tau) = \sum_{k=1}^{M-1} A_k Z_n^{(k)} \mu_k^{\tau}, \tag{F24}$$

where

$$\mu_k = C\lambda_k + (1 - C) \tag{F25}$$

and where ψ_n, λ_k and $Z_n^{(k)}$ are given by Eqs. (C5), (C16), and (C17). Again, from Eqs. (F23) and (F25)

$$\lim_{F\to\infty} \mu_k = \lambda_k, \tag{F26}$$

and Eq. (F24) reduces to our previous result, Eq. (C19).

Assuming that the initial phase distribution is given by Eq. (C2) (cf. also Fig. 5) the expansion coefficients A_k in Eq. (F24) are once again given by Eq. (C23). Analogous to Eqs. (C24) and (C25) we now obtain

$$\psi_n(\tau) = \sum_{k=1}^{M-1} \psi_n^{(k)}(\tau), \tag{F27}$$

where

$$\psi_n^{(k)}(\tau) = [\Delta\theta_n(\infty) - \Delta\phi_0](-1)^k \cot\left(\frac{\pi k}{2M}\right) \sin\left(\frac{\pi kn}{M}\right)\left[1 - 2C \sin^2\left(\frac{\pi k}{2M}\right)\right]^{\tau}. \tag{F28}$$

Equation (F27) is the exact solution of the phase-diffusion equation, Eq. (F22). However, Eq. (F22) is itself only an approximation to Eq. (F1), valid in the limit $\tau >> 1$. Thus, even if all $(M-1)$ terms are kept in our expansion for $\psi_n(\tau)$, Eq. (F27), the result is still just an approximation. By contrast, Eq. (C24) provides the exact solution to Eq. (C1).

Another distinction between Eqs. (F27) and (C24) is in the eigenvalue spectrum that determines the time-dependence of the space/time modes, $\psi_n^{(k)}(\tau)$. Previously, we found that the k-mode was degenerate with the $(M-k)$-mode, i.e., that

$$|\lambda_k| = |\lambda_{M-k}|. \tag{F29}$$

Consequently, it was necessary to retain the highly oscillatory $(M-1)$-mode in developing an approximation to Eq. (C24). However, we now find that self-coupling has broken the degeneracy,

$$|\mu_k| > |\mu_{M-k}|, \tag{F30}$$

and that we need retain only the slowly varying $k = 1$ term in developing an approximation to Eq. (F27). Assuming that $(\pi/M) << 1$,

$$\hat{\theta}_n(\tau) = \theta_n(\infty) - (2M/\pi)[\Delta\theta_n(\infty) - \Delta\phi_0] \sin(n\pi/M) e^{-\tau/T_s}, \tag{F31}$$

analogous to Eq. (33). However, we now have a different value for the settling time,

$$T_s = \tau_s\left(1 + \frac{1}{2} F^{-1} \sec\Delta\phi\right), \tag{F32}$$

where $\tau_s = M^2/5$ is the settling time for modules without self-coupling, Eq. (34). In general, when $F > 0$, stable equilibrium phase distributions must have $0 \leqslant \Delta\phi < \pi/2$; when $F < 0$, we have $\pi/2 \leqslant \Delta\phi < \pi$. It then follows from Eq. (F32) that

$$T_s \geqslant \tau_s, \tag{F33}$$

always; i.e., modules without self-coupling settle faster than modules with self-coupling.

Instead of Eq. (35) we now obtain

$$\Delta\hat{\theta}_n(\tau) = \Delta\theta_n(\infty) - 2[\Delta\theta_n(\infty) - \Delta\phi_0] \cos(n\pi/M) e^{-\tau/T_s}, \tag{F34}$$

where T_s is once again given by Eq. (F32). Comparing the n-dependence of Eqs. (35) and (F34) we see that Eq. (F34) is missing the highly oscillatory factor μ that represents the contribution of $\psi_n^{(M-1)}$ to Eq. (35).

We have compared the one-mode approximation, Eq. (F34), with some exact computer solutions to Eq. (F1). In performing these calculations we assume that

$$(M,\ \Delta\phi_0,\ \alpha_M(0)) = (9,\ 60°,\ 45°) \tag{F35}$$

as for Eq. (36) and Fig. 8. Figure F1 presents a comparison between the analytic and numerically derived phase distributions as a function of the module index n for two particular values of time ($\tau = 70$ and $\tau = 100$).

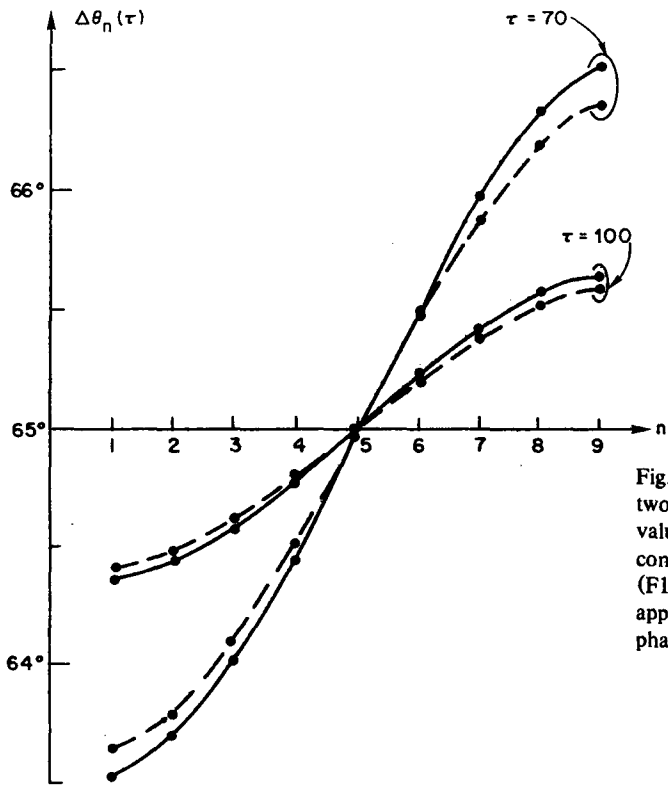

Fig. F1 — Phase distribution for a self-coupled 8-module feed at two values of time ($\tau = 70$ and $\tau = 100$). Assumed parameter values are $(M, \Delta\phi_0, \alpha_M(0), F) = (9, 60°, 45°, 1)$. Phase values connected by solid lines obtained by numerical solution of Eq. (F1); values connected by dashed lines obtained by one-mode approximation, Eq. (F34). In the infinite-time limit a uniform phase gradient is established, $\Delta\theta_n(\infty) = \Delta\phi = 65°$.

Compared with Fig. 8 we note from Fig. F1 that the phase distribution for self-coupled modules evolves much more slowly with time and is spatially smoother than the phase distribution of modules that lack self-coupling.